

**CEREBROVASCULAR DYNAMICS IN MIGRAINE MEASURED
WITH fNIRS**

by

Didem Bilensoy

B.S., Electrical & Electronics Engineering, Boğaziçi University, 2003

Submitted to the Institute of Biomedical Engineering
in partial fulfillment of the requirements for the degree of
Master of Science
in
Biomedical Engineering

Boğaziçi University

2005

**CEREBROVASCULAR DYNAMICS IN MIGRAINE MEASURED
WITH fNIRS**

APPROVED BY:

Assist. Prof. Dr. Ata Akın
(Thesis Supervisor)

Assoc. Prof. Dr. Yasemin Kahya

Assoc. Prof. Dr. Hale Saybaşılı

DATE OF APPROVAL: 16.06.2005

ACKNOWLEDGEMENTS

First of all, I would like to thank my supervisor Dr. Ata Akin who has guided and supported me generously during my studies. I am grateful to him for his valuable contributions to my project and also proof reading my M.S. thesis.

I would like to express my gratitude's to Uzay Emrah Emir and Murat Tümer who made the experimental measurements possible by developing the fast optical imager, NIROSCOPE 201.

I am thankful to Dr. Hayrunnisa Bolay for her collaboration and her help on providing data from migraineurs subjects.

Last, but not least, I would like to thank my parents and my spouse who have always supported and encouraged me.

ABSTRACT

CEREBROVASCULAR DYNAMICS IN MIGRAINE MEASURED WITH fNIRS

Migraine is a neurovascular pain syndrome affecting nearly 12 per cent of world's population. Migraine decreases the life quality and work efficiency of patients drastically, and causes billions of dollars of economical loss to countries. Therefore, accurate diagnosis and treatment of migraine is important which is only possible by understanding its dynamics.

This study aims to observe the differences cerebrovascular dynamics of migraine patients and healthy subjects by measuring their cerebrovascular responses during breath hold task by using functional near infrared spectroscopy. The subjects' responses are modeled using Gaussian functions and the obtained model parameters of migraineurs and healthy subjects are compared. All amplitude parameters of migraineurs were found to be approximately half of those for healthy subjects supporting that migraineurs' responses are suppressed for not only Hb dynamics but also HbO₂ dynamics. Moreover, migraineous responses were found to be unpredictable as opposed to healthy subjects suggesting that migraineurs have an inherent incapability for cerebral autoregulation. Time to peak values of migraineurs' Hb are found to precede the healthy subjects at least eight seconds while their HbO₂ values lagged around nine seconds. Our findings indicate that regulation of cerebral dynamics of migraine patients during breath hold task is significantly different than the healthy subjects.

Keywords: Migraine, Cerebrovascular Dynamics, Functional Near Infrared Spectroscopy (fNIRS), Gaussian function.

ÖZET

İŞLEVSEL YAKIN KIZIL ÖTESİ SPEKTROSKOPİ İLE ÖLÇÜLMÜŞ MİGREN SEREBROVASKÜLER DİNAMİKLERİ

Migren dünya nüfusunun yaklaşık yüzde 12'sini etkileyen nörovasküler bir ağrı sendromudur. Migren, hastaların yaşam kalitelerini ve verimliliklerini ciddi ölçülerde etkilerken, ülke ekonomilerine de milyonlarca dolar zarar vermektedir. Bu sebeplerden dolayı hastalığın doğru teşhisi ve tedavisi önem kazanmaktadır; bu da ancak migren dinamiklerinin daha iyi anlaşılması ile mümkündür.

Bu çalışma migren hastalarının ve sağlıklı deneklerin serebrovasküler dinamikleri arasındaki farkları nefes tutma sırasında serebrovasküler dinamikleri yakın kızıl ötesi spektroskopisi kullanarak gözlemlemeyi amaçlamaktadır. Kullanılan yöntem ardı ardına tutulan dört nefese deneklerin verdiği tepkilerin işlevsel yakın kızıl ötesi spektroskopisi ile ölçülmesi şeklindedir. Deneklerin tepkileri gauss fonksiyonu kullanılarak modellenmiş ve elde edilen model parametreleri migrenli ve sağlıklı denekler için karşılaştırılmıştır. Hem Hb hem de HbO₂ dinamiklerinin migrenliler için bastırılmış olduğu görüşünü destekler biçimde migrenlilere ait tüm genlik parametrelerinin, sağlıklı deneklerin parametrelerinin yaklaşık yarısına eşit olduğu gözlenmiştir. Ayrıca migrenlilerin serebral otoregülasyon yetersizliğini işaret eder biçimde, migrenlilerin yanıtlarının sağlıklı deneklerin aksine önceden bilinemez olduğu görülmüştür. Migrenlilerin Hb yanıtında tepe noktası zamanı değerleri sağlıklı deneklerden en az sekiz saniye önceden gelmekte, HbO₂ yanıtında ise yaklaşık dokuz saniye gecikmektedir. Bulgularımız migrenlilerde nefes tutma sırasında serebral dinamiklerin regülasyonunun sağlıklı deneklerden önemli şekilde farklı olduğunu göstermektedir.

Anahtar Sözcükler: Migren, Serebrovasküler Dinamikler, İşlevsel Yakın Kızılötesi Spektroskopisi, Gauss Fonksiyonu.

TABLE OF CONTENTS

ACKNOWLEDGEMENTS.....	iii
ABSTRACT.....	iv
ÖZET.....	v
LIST OF FIGURES.....	viii
LIST OF TABLES.....	x
LIST OF SYMBOLS.....	xi
LIST OF ABBREVIATIONS.....	xii
1. INTRODUCTION.....	1
1.1 Motivation and Objectives.....	1
1.2 Outline.....	1
2. MIGRAINE.....	3
2.1 Migraine: Symptoms and Course.....	4
2.2 Migraine: Diagnosis and Classification.....	5
2.3 Pathophysiology of Migraine.....	7
2.3.1 Trigeminal Nerve.....	8
2.3.2 The Vascular Theory.....	10
2.3.3 The Cortical Spreading Depression (CSD) Theory.....	10
2.3.4 The Neurovascular Hypothesis.....	12
2.3.5 The Serotonergic Abnormalities Hypothesis.....	13
2.3.6 The Unifying Theory.....	14
3. IMAGING MIGRAINE.....	15
3.1 Functional Near Infrared Spectroscopy (fNIRS).....	15
3.2 fNIRS in Cerebral Metabolism and Neurodynamics.....	17
4. METHOD.....	19
4.1 Experimental Protocol.....	19
4.2 Data Collection.....	20
4.3 Preprocessing Data.....	21
4.4 Function Adaptation and Nonlinear Regression to [Hb] and [HbO ₂] Signals.....	22
4.4.1 Gaussian Function.....	22

4.4.2 Nonlinear Regression.....	23
4.5 Data Processing and Curve Fitting.....	25
5. RESULTS AND DISCUSSION.....	28
5.1 Amplitude (A).....	32
5.1.1 [Hb] Signal Amplitudes.....	33
5.1.2 [HbO ₂] Signal Amplitudes.....	35
5.2 Time to Peak (D).....	38
5.3 Dispersion (τ).....	40
6. CONCLUSIONS.....	41
6.1 Recommendations for Future Work.....	41
APPENDIX A. SCATTER GRAPHICS.....	42
REFERENCES.....	46

LIST OF FIGURES

Figure 2.1	The meninges [4].....	4
Figure 2.2	Trigeminal nerve [16].....	9
Figure 2.3	Dilation in trigeminovascular system [19].....	9
Figure 2.4	Cortical spreading depression (1) Spreading wave of cortical hyperexcitability, (2) CSD area suppressed neurological activity trailing the wave, (3) Area of normal brain activity, (4) Progression of the wave, (5) Expansion of the CSD area, (6) Area of CSD progressed from the occipital lobe, until terminated [28].....	11
Figure 2.5	Trigeminovascular system activation and vasodilation [15].....	13
Figure 3.1	(a) Absorption spectrum of chromophores (b) The model of neuroimaging [36].....	16
Figure 4.1	The breath holding protocol.....	19
Figure 4.2	NIROXCOPE 201 probe spatial optode locations, optode number 1 being on the left top of the forehead.....	20
Figure 4.3	Photograph of the functional optical imager, NIROXCOPE 201 [36].....	21
Figure 4.4	A representation of the brain hemodynamic response as the summation of three modified gaussian functions ($A_1 = -0.30$, $A_2 = 0.75$, $A_3 = -0.25$, $D_1 = 20$, $D_2 = 45$, $D_3 = 75$, $\tau_1 = 11$, $\tau_2 = 7$, $\tau_3 = 6$).....	23
Figure 4.5	Preprocessed $[Hb]$ and $[HbO_2]$ data during breath hold experiment for (a) a healthy subject and (b) a migraineur (Vertical lines indicate the beginning and end of the breath holding. True values for Hb and HbO_2 data are in μM).....	26
Figure 4.6	Actual $[Hb]$ data and its nonlinear regression curve fit from a (a) healthy subject and a (b) migraine patient (The smooth lines are the fit to real data).....	27
Figure 5.1	Statistically significant data with $p = 0.002$, according to ANOVA analysis.....	28
Figure 5.2	Examples for ANOVA analysis with 2 different data sets; first one being statistically significant with (a) $p = 0.0291$ and the other having no diagnostic value (b) $p = 0.5878$	29

Figure 5.3	Real Hb and HbO ₂ data with standard deviations obtained for (a) healthy subjects and (b) migraineurs with mean values shown as the lines passing through error bars.....	30
Figure 5.4	Real data with standard deviations obtained from healthy subjects and migraineurs (a) [Hb] (b) [HbO ₂] with mean values shown as the lines passing through error bars.....	31
Figure 5.5	Constructed [Hb] dynamics using the estimated parameters for healthy subjects and migraineurs in comparison	32
Figure 5.6	Constructed [HbO ₂] dynamics using the estimated parameters for healthy subjects and migraineurs in comparison.....	32
Figure 5.7	Mean amplitude (<i>A</i>) values of [<i>Hb</i>] signal of healthy subjects and migraineurs in μM	34
Figure 5.8	Mean amplitude (<i>A</i>) values of [<i>HbO</i> ₂] signal of healthy subjects and migraineurs in μM	37
Figure 5.9	Estimated [<i>Hb</i>] and [<i>HbO</i> ₂] dynamics of (a) healthy subjects and (b) migraineurs.....	39
Figure A.1	[Hb] signal initial response scatter graphics for four consecutive breath holds from all subjects.....	42
Figure A.2	[Hb] signal (a) main response and (b) recovery response scatter graphics for four consecutive breath holds from all subjects.....	43
Figure A.3	[HbO ₂] signal (a) initial response and (b) main response scatter graphics for four consecutive breath holds from all subjects.....	44
Figure A.4	[HbO ₂] signal recovery response scatter graphics for four consecutive breath holds from all subjects.....	45

LIST OF TABLES

Table 5.1	Amplitude (A) values of averaged [Hb] signal for four breath holds.....	33
Table 5.2	Amplitude (A) values of [Hb] signal for groups of the mean values of the four breath holds.....	34
Table 5.3	Amplitude (A) values of [Hb] signal for consecutive breath holds.....	35
Table 5.4	Percentage changes between breath holds in [Hb] amplitude (A).....	35
Table 5.5	Amplitude (A) values of averaged [HbO_2] signal for four breath holds.....	36
Table 5.6	Amplitude (A) values of [HbO_2] signal for groups of the mean values of the four breath holds.....	36
Table 5.7	Amplitude (A) values of [HbO_2] signal for consecutive breath holds.....	37
Table 5.8	Percentage changes between breath holds in [HbO_2] amplitude (A).....	38
Table 5.9.	Time to peak (D) values of averaged signals for four breath holds.....	39
Table 5.10	Dispersion (τ) values of averaged signals for four breath holds.....	40

LIST OF SYMBOLS

A	Amplitude
A_1, A_2, A_3	Amplitude parameters of initial, main and recovery phases
d	Source-detector distance
D	Time to peak
D_1, D_2, D_3	Time to peak parameters of initial, main and recovery phases
f	Predefined function
Hb	Deoxy-hemoglobin
HbO ₂	Oxy-hemoglobin
I	Output light intensity
I_0	Input light intensity
x	Covariate vector
Y	Response
ε	Random error
μ	Medium absorption coefficient
θ	Parameter vector
σ	Differential path length factor
τ	Dispersion
τ_1, τ_2, τ_3	Dispersion parameters of initial, main and recovery phases

LIST OF ABBREVIATIONS

BHR	Brain Hemodynamic Response
CGRP	Calcitonin Gene Related Peptide
CSD	Cortical Spreading Depression
CT	Computed Tomography
EEG	Electroencephalography
FHM	Familial Hemiplegic Migraine
fMRI	Functional Magnetic Resonance Imaging
fNIRS	Functional Near Infrared Spectroscopy
IHS	International Headache Society
MRI	Magnetic Resonance Imaging
NIRS	Near Infrared Spectroscopy
PET	Positron Emission Tomography
REM	Rapid Eye Movement

1. INTRODUCTION

1.1. Motivation and Objectives

Migraine is a neurovascular disorder, believed to affect nearly 12 per cent of the world's population. Migraine decreases the life quality of the patients drastically by knocking them out during attacks and forces them to restrict their daily activities between the attacks such as exercising, working, eating and sleeping in a way to avoid more frequent attacks. The disabling property of migraine also costs billions of dollars of economical loss to countries annually. Therefore, accurate diagnosis and treatment of migraine is important, which is only possible by understanding its dynamics [1, 2].

This study aims to observe the cerebrovascular dynamics of migraine patients and find out the differences between their and the healthy subjects' dynamics. It is intended to represent the dynamics of migraineurs and healthy subjects with the most suitable mathematical model and compare the model parameters in order to obtain concrete diversities between the subject groups. A possible use of distinguishable parameters for migraineurs and healthy subjects will be migraine diagnosis. Although migraine has very unique symptoms, before diagnosing a person with migraine several test are applied in order to rule out a secondary headache causing migraine-like complaints which is not rare. These tests include but are not limited to general physical and neurological exams and for suspicious cases very expensive laboratory and radiological tests. Thus data from cerebrovascular dynamics confirming that a patient has migraineous response may at least decrease the need for costly examinations.

1.2 Outline

In this study, topics that are mandatory to understand the cerebrovascular dynamics of healthy people and migraine patients, and detect the hypothesized differences between them are attempted to be covered. Basic knowledge of migraine physiology and imaging

techniques, application of mathematical methods and data analysis constitute the guidelines of the thesis.

Chapter 2 contains the essential information about migraine. The symptoms and the course of migraine is the first subsection of the chapter, followed by the diagnostic criteria and the classification of migraine types. The migraine pathophysiology is the subject of the final subsection. A short introduction to the key element of migraine, trigeminovascular system, is followed by the discussion of the most commonly referred theories of migraine pathogenesis.

Chapter 3 begins with a quick review of the imaging methods that are used for neuroimaging, especially for headache diagnosis and studies including migraine. Then the working principle of the fast optical imaging system that is used to gather data, functional near infrared spectroscopy, is acquainted briefly. Chapter 3 ends with a state of art subsection about the usage of near infrared spectroscopy in cerebral metabolism and neurodynamics.

Experimental protocol applied, methods and device used during data collection are mentioned in Chapter 4. Preprocessing procedure to prepare data for analysis, the function of choice to represent the cerebrovascular dynamics and regression technique applied are the other topics this chapter covers. Final subsection focuses on the data processing and curve fitting, which will provide the results for the thesis.

The results of the study are presented in Chapter 5. Responses and parameters obtained are compared among the healthy subjects and migraineurs. The characteristics of the dynamics for each group and their differences are also discussed in this chapter.

Chapter 6 provides a general discussion of the analysis done and proposes possible improvements for future work that may lead to better results.

2. MIGRAINE

The brain itself is known to be mostly insensitive to pain but meninges which enclose and protect the central nervous system is one of the few pain sensitive tissues in the cranium [3]. Three different connective tissue membranes, namely dura mater, arachnoid and pia mater constitute the meninges. The dura mater is the thickest and the outermost part of the meninges, dividing into two layers; external and internal layers. Internal layer of the dura mater, also called cranial dura mater, is the true meningeal dura mater. Although it is adherent to the external layer in most places, structures such as the dural sinuses and the trigeminal cave are formed from the separation of these two layers. Arachnoid is the avascular membrane lying underneath the dura mater. Between dura mater and arachnoid there is a subdural space responsible for keeping the two membranes lubricant. Pia mater is the most delicate and vascular part of the meninges and adherent to the central nervous system, enclosing it (Figure 2.1). Therefore, it can be concluded that, when a headache is experienced, it is either, due to any damage to the tissues covering the brain, the structures attached to the base of the brain or due to an abnormality of the blood vessels and muscles surrounding the scalp, face and neck, causing it [4].

Headaches are roughly grouped as primary and secondary headaches. A headache is considered to be primary if its cause is not another disease or medical condition. Otherwise, if the headache is the result of another medical condition such as neck injuries, infections in nasal and sinus passages, the headache is defined to be a secondary headache. Secondary headaches account for only two per cent of all headaches. Primary headaches have three main types. Tension headaches are the most common type, constituting nearly 90 per cent of all headaches. Migraine is the second common type of primary headaches, followed by the cluster headaches according to the frequency of occurrence [5].

Migraine is a neurovascular pain syndrome, affecting nearly 12 per cent of the population, mostly women. Migraine is characterized by four to seventy two hour-lasting attacks, with the most distinguishable symptom, throbbing pain on one side of the head, in fact, the word migraine has originated from the Greek word hemicrania, meaning “half of

the head”. Aggravation of pain by routine physical activity, extreme sensitivity to light, noise and smell, nausea and vomiting are other common symptoms of migraine.

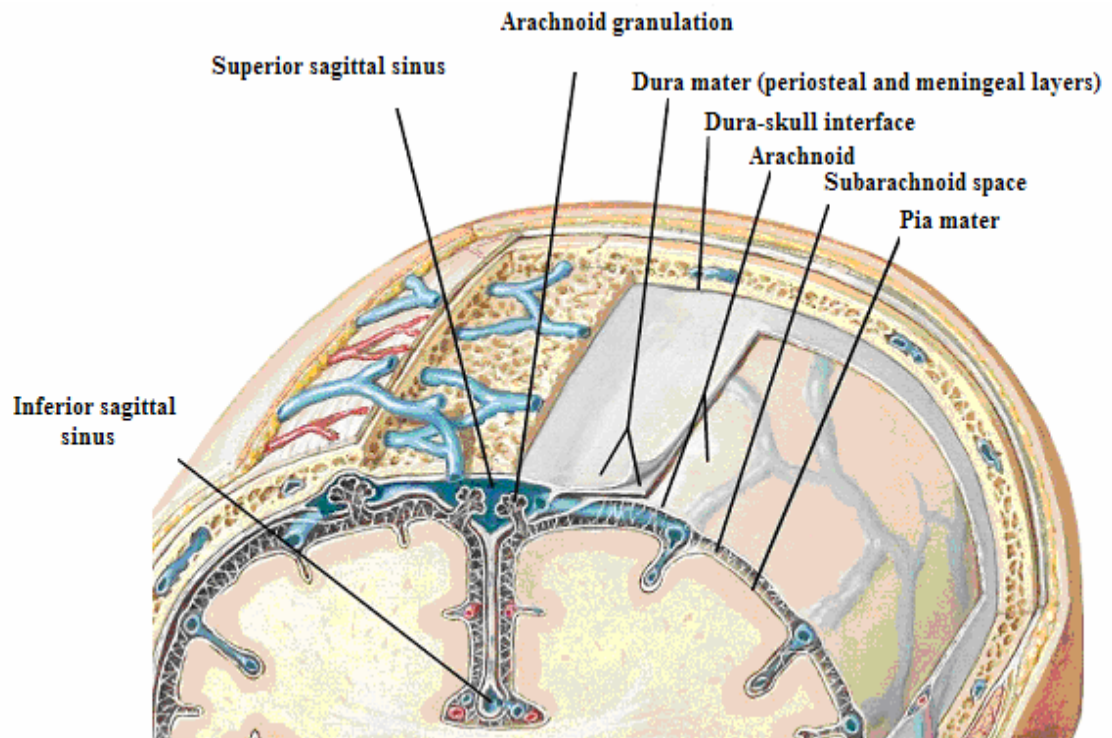


Figure 2.1 The meninges [4].

2.1 Migraine: Symptoms and Course

Although not observed exactly by every migraineur, a migraine episode generally has four phases; the prodrome, the aura, the attack and the postdrome. The prodrome phase may exhibit symptoms such as mood changes, fatigue, yawning, reduced appetite or food cravings which may start a few hours or days before the attack. The prodrome is followed by the aura phase, which is mainly the sensory disturbances before the attack, experienced by less than 20 per cent of migraineurs. Most of the time aura stage is characterized by visual disturbances such as bright lights and shapes, zigzag lines, blind spots and tunnel vision, although various neurological disturbances, namely, confusion, numbness and weakness in arms or legs, difficulty in some cognitive processes including speech and perception may also be observed. The attack is the phase which patients suffer from the signature symptoms of migraine, pulsating unilateral pain, photophobia, phonophobia, osmophobia, sensitivity to motion, nausea and rarely vomiting. This phase may last from

four hours to seventy two hours. The postdrome is the after attack phase, during which patients usually feel exhausted, but start to recover and crave for food [2, 6].

2.2 Migraine: Diagnosis and Classification

Migraine affects about eighteen per cent of women and six percent of men, having the peak prevalence between the ages 25 and 55, corresponding the period of maximum productivity in human life; both decreasing the life quality and work efficiency of patients, causing billions of dollars economical loss to countries. These facts about migraine make early diagnosis and correct treatment important. Because of the incomplete knowledge of its pathophysiology and absence of specific markers in its course, up to now, migraine diagnosis had to be based on the diagnostic criteria, in the international classification derived from clinical and epidemiological data [7].

Aretaeus of Cappadocia (AD 30-90), introduced the earliest known comprehensive classification of primary headaches and separated migraine calling it heterocrania, according to the symptoms he identified, such as unilateral nature, blackness before eyes (aura symptom), nausea, photophobia, from cephalalgia (not very severe, short-lasting) and cephalaea (intense, chronic, frequent). He successfully described unilateral pain ("the pain... remains in the half of the head"), photophobia and phonophobia ("For they flee the light; the darkness soothes their disease; nor can they bear readily to look upon or hear anything disagreeable") in his own terms. He also determined the life span of heterocrania, to be from several hours to a day, by saying "If they begin at dusk, they end by midday on the next day, and if they begin at midday, they end by nightfall. It is rare for the attack to last longer" [8, 9].

International Headache Society (IHS) had published diagnostic criteria for the most common migraine types, migraine with aura and migraine without aura in 1988. Migraine with aura, also known as classic migraine, accounts for less than 20 per cent of migraines, and has subcategories such as migraine with typical aura, migraine with prolonged aura, familial hemiplegic migraine (FHM), basilar migraine, migraine aura without headache and migraine with acute onset aura. Rest of the migraineurs, constituting nearly 80 per cent

of migraine sufferers, have migraine without aura, also called common migraine. According to IHS, a person may be diagnosed with migraine without aura, if he had at least five attacks lasting four to seventy two hours (untreated or unsuccessfully treated), which has at least two of the four following characteristics: unilateral location, pulsating quality, moderate or severe intensity (inhibits or prohibits daily activities) and aggravated by walking stairs or similar routine physical activity. Furthermore, during the headache at least one of these symptoms should occur: phonophobia and/or photophobia, nausea and/or vomiting. In addition to the migraine without aura criteria, diagnosis of migraine with aura requires the history of at least two attacks fulfilling at least three of the following: one or more fully reversible aura symptoms indicating focal cerebral cortical and/or brain stem functions, at least one aura symptom develops gradually over more than four minutes, or two or more symptoms occur in succession, no aura symptom lasts more than 60 minutes; if more than one aura symptom is present, accepted duration is proportionally increased, headache follows aura with free interval of less than 60 minutes. Moreover, at least one of the following aura features establishes a diagnosis of migraine with typical aura: homonymous visual disturbance, unilateral paresthesias and/or numbness, unilateral weakness, and aphasia or unclassifiable speech difficulty [6].

In order to make an accurate migraine diagnosis, knowledge of clinical history, physical and neurological examinations are necessary. Clinical history is used for better specificity and sensitivity to IHS criteria, either favorable or unfavorable for migraine diagnosis. For example, presence of family history of migraine, motion sickness history, reaction to triggers strengthens the suspicion that a patient has migraine, while factors such as, changing pain features, constantly worsening pain, association with systemic symptoms, and new on set after 45 years of age are unfavorable, being usually signs of a secondary headache, and requires further investigation for making a migraine diagnosis. After reviewing clinical history, general and neurological examinations must be performed and appropriate laboratory and radiological test should be requested, in order to eliminate all possible forms of secondary headaches that are stated before. A complete general physical examination is done, including checking patient's blood pressure, heart rate, body temperature, paranasal sinuses, cervical and paraspinal muscles, and temporomandibular joints. Physical examination followed by a neurological examination, focusing on any impairment on the level of consciousness, presence of meningeal irritation, focal signs and

abnormalities in optic fundi. Depending on the results of the general examinations, further tests may be performed when clinical suspicion needs their utility. Using neuroimaging for the patients with neurological signs is a standard procedure, according to that approach [10-12].

2.3 Pathophysiology of Migraine

Although it is known to be mostly insensate, the brain has a pain system to signal tissue injury like other organs; trigeminovascular system acts as a warning system, causing migraines to help "protect" the brain against insults such as ischemia, toxins, and intrinsic disease. It has been suggested that it is theoretically possible for all individuals to suffer a migraine attack. The occurrence and frequency of attacks in any individual will be governed by the sensitivity of their central nervous system to migraine specific triggers (e.g. certain foods, hormones, changes in levels of stress, consciousness and even exposure to light, sound and smell). It has been hypothesized that genetic abnormalities result in a lowered threshold of response to these specific trigger factors in migraineurs. The trigger factors can thus be conceptualized as modulators of the genetic set point that predisposes to migraine. Conversely, in normal individuals, who lack genetic deficits relevant to migraine, exposure to the same trigger factors would not breach the 'migraine threshold' and so an attack would not be initiated. It is possible that the abnormal hyperresponsivity of the brain of migraineurs, like FHM, may be a consequence of genetic abnormalities in ion channels that regulate neuronal excitability [13]. That sensitivity causes some scientists to identify migraine with a smoke alarm that will reliably wake a sleeping family in the event of any fire, giving false alarms every time the toast burns [14].

Although exact mechanisms underlying migraine remain uncertain, several theories have been proposed. Various facts and observations about the disease acquired from both migraine research and clinical experiences have been the starting point for these hypothesis. Some essential information about migraine gathered by these studies and widely used by scientists to form hypothesis, are the following, migraine:

- May be triggered by factors such as diet, sleep and hormonal changes.

- Has a circadian rhythm similar to several diseases of vasoconstriction.
- May be aborted by sleep.

Other important data obtained during migraine episodes includes decreased cerebral blood flow during the aura phase, generalized systemic vasoconstriction and local cerebrovascular vasodilation at the side of headache, serotonin release from platelets during the migraine attack, and increased calcitonin gene-related peptide (CGRP) and substance P levels during attack [15].

Prior to reviewing the theories and hypothesis about migraine pathophysiology, the trigeminal nerve, which plays important roles in these models, will be mentioned briefly.

2.3.1 Trigeminal Nerve

The trigeminal nerve is the fifth of the cranial nerves and is denoted by the Roman number V. It inherited its name from the Latin trigeminus meaning “threefold” referring to its three divisions; ophthalmic (V1, sensory), maxillary (V2, sensory), and mandibular (V3, motor and sensory). The trigeminal nerve is the facial touch, temperature and pain sensor. In addition to its sensory functions, the mandibular division also controls chewing activity. Within the ophthalmic and maxillary sensory nerves, there are also meningeal sensory branches that enter the trigeminal ganglion within the cranium. The sensory part of the mandibular nerve is composed of branches that carry general sensory information from the mucous membranes of the mouth and cheek, anterior two-thirds of the tongue, lower teeth, skin of the lower jaw, side of the head and scalp, and meninges of the anterior.

The area the three branches of trigeminal nerve come together is called Gasserion ganglion (Figure 2.2). After the ganglion the trigeminal nerve root continues back towards the side of the brain stem, and inserts into the pons. Within the brain stem, the signals traveling through the trigeminal nerve reach specialized clusters of neurons called the trigeminal nerve nucleus. Information brought to the brain stem by the trigeminal nerve is then processed before being sent up to the brain and cerebral cortex, for higher order processing [16, 17].

Trigeminal nerve may be stimulated by both neuronal and chemical triggers. Chemical activators such as fluctuating estrogen levels, low blood sugar, chemicals found in certain foods works directly on nerve stimulation, while neuronal activators usually work indirectly such as REM sleep related serotonin release.

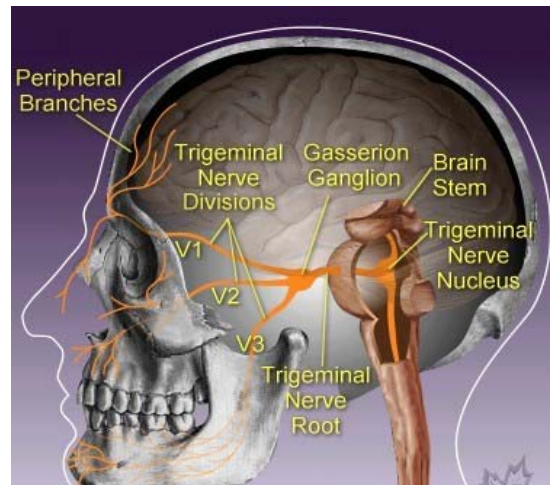


Figure 2.2 Trigeminal nerve [16].

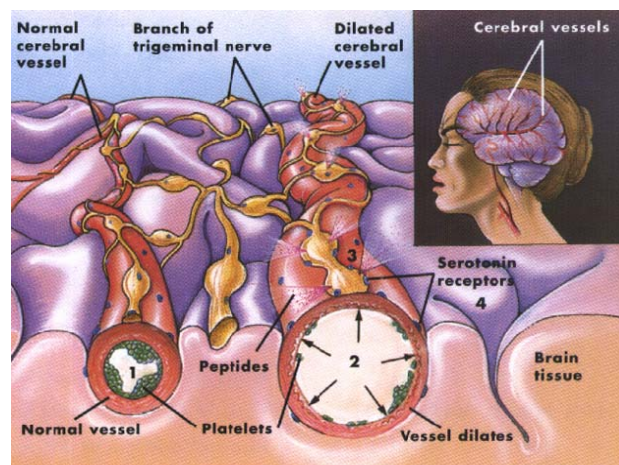


Figure 2.3 Vessel dilation in trigeminovascular system [19].

Small calibrated trigeminal axons innervate meninges, some of which bifurcate in proximity to small blood vessels branching from pial and dural arteries. They contain vasoactive neuropeptides (such as substance P, CGRP and neurokinin A) that promote plasma protein leakage and vasodilation within dura mater characteristic of neurogenic inflammation when released. Upon stimulation of vessels in humans, pia and dura mater generate throbbing unilateral pain, hence the term trigeminovascular system was coined [3,

18]. Trigeminovascular system will be mentioned again as a part of the neurovascular and integrated hypothesis of migraine subsections of this section.

2.3.2 The Vascular Theory

The vascular theory, the oldest approach to understand migraine as proposed in 1938 by Graham and Wolff, claims that migraine is a vasospastic disorder and attributes it to an initial intracranial arterial vasoconstriction, resulting in reduced blood flow to the visual cortex, followed by a period of extracranial vasodilation [20].

The studies investigating effects of vasodilators and vasoconstrictors on both migraineurs and healthy subjects support the claims of the vascular theory [21]. It is proved that vasodilators such as nitric oxide may induce a headache and if introduced during a migraine attack worsen the pain subject experiences. Furthermore, using vasoconstrictor medication, serotonin or oxygen which may also act as vasoconstrictor during attack improves or aborts headache. Usage of vasoconstrictors by migraineurs for alleviating pain is a controversial issue today; however it is still commonly practiced.

The development of new technologies allow scientist to investigate the vascular dynamics and the long standing theory more closely. Research has shown that during a migraine attack without aura, there are in fact only minor changes in cerebral blood flow, and the proposed initial vasoconstrictive phase may actually last several hours longer than the aura. It is also hypothesized that migraine sufferers have an inherent vasomotor instability and are more susceptible to the vasodilatory effects of certain chemical and physical agents [22]. Moreover, the vascular theory remains incapable of explaining the local swelling and tenderness of the head by only vasodilation [15].

2.3.3 Cortical Spreading Depression (CSD) Theory

Cortical spreading depression (CSD) is a migrating inactivation of gray matter first described by Leao [23] that can be focally induced by mechanical, electrical, or chemical stimulation under normal metabolic conditions. The propagating wave of depolarization

and associated electrical silence spreads across the cerebral cortex at two to five mm/min moving from occipital region towards the front. CSD is thought to be responsible for migraine aura, commonly a marching visual or somatosensory deficit that may precede migraine pain [24]. The mass depolarization of neurons and glia CSD involves is shown to last about a minute without causing any known neuronal damage [25, 26].

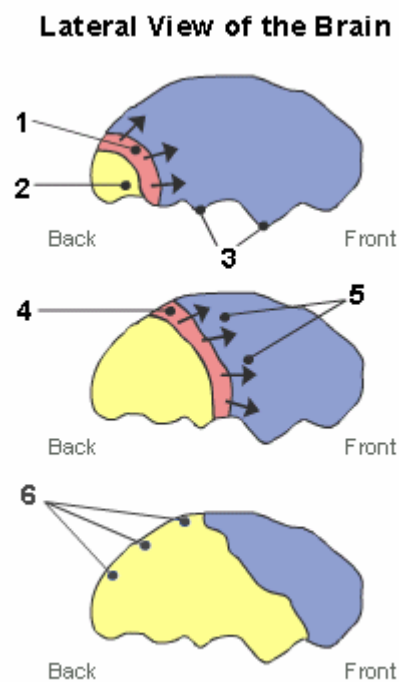


Figure 2.4 Cortical Spreading Depression (1) Spreading wave of cortical hyperexcitability, (2) CSD area suppressed neurological activity trailing the wave, (3) Area of normal brain activity, (4) Progression of the wave, (5) Expansion of the CSD area, (6) Area of CSD progressed from the occipital lobe, until terminated [27].

According to the CSD theory, the prolonged neuronal depression after the short excitation wave causes disturbances in both nerve cells and regional blood flow [15]. Migraine aura, especially the visual disturbances migraineurs suffer, are attributed to the spreading wave that is suppressing the neuronal activity, unlike the vascular theory explaining aura phase with the vasoconstriction related purposes. Support for CSD theory comes from migraine with aura studies, which conclude that progression rate of the excitation wave is followed by a similar rate of reduced blood flow [28].

2.3.4 The Neurovascular Hypothesis

As described in subsection 2.3.1, the trigeminal nerve fibers innervate several blood vessels including the ones in the meninges, and the extracranial arteries. Primarily the ophthalmic division of the trigeminal nerve innervates the meninges. The trigeminal nerves arise from pseudo-unipolar neurons in the trigeminal ganglia and project to the intracranial extracerebral blood vessels in the meninges (peripheral terminals) and behind the blood brain barrier into the trigeminal nuclei in the brain stem and upper cervical spinal cord (central terminals). These fibers therefore provide a pathway for pain signal transmission from meningeal blood vessels into the brain where headache pain is registered. This system has been described collectively as the trigeminovascular system [13].

The nerve fibers of the trigeminal nerve contain nociceptors that are capable of generating pain impulses, and the endings of these nerve fibers contain peptide neurotransmitters. It is proposed that either migraine triggers or CSD can activate trigeminal nerve axons, which then release neuropeptides (such as substance P, neurokinin A and CGRP) from axon terminals near the meningeal and other blood vessels (Figure 2.5).

Substance P and neurokinin A are known to cause vasodilation and promote the extravasation of plasma proteins and fluid from nearby meningeal blood vessels. Similarly, CGRP is a potent vasodilator but it does not lead to plasma extravasation. The produced inflammation is termed sterile neurogenic perivascular inflammation. The neuropeptides may also sensitize nerve endings, providing a mechanism for sustaining the headache. The stimulated trigeminal nerve also transmits pain impulses to the trigeminal nucleus caudalis, which relays pain impulses to higher centers of the brain. Neurovascular theory claims that vasodilation is not the cause but an accompanying phenomenon to migraine attributable to trigeminal nerve activation [15].

Some of the studies supporting the neurovascular theory propose that in migraineurs, genetic abnormalities cause an inability to handle migraine trigger factors adequately and result in a primary neural dysfunction within the central nervous system. Indeed, studies have shown that the brain of migraineurs has altered responsivity to transcranial magnetic stimulation [29, 30].

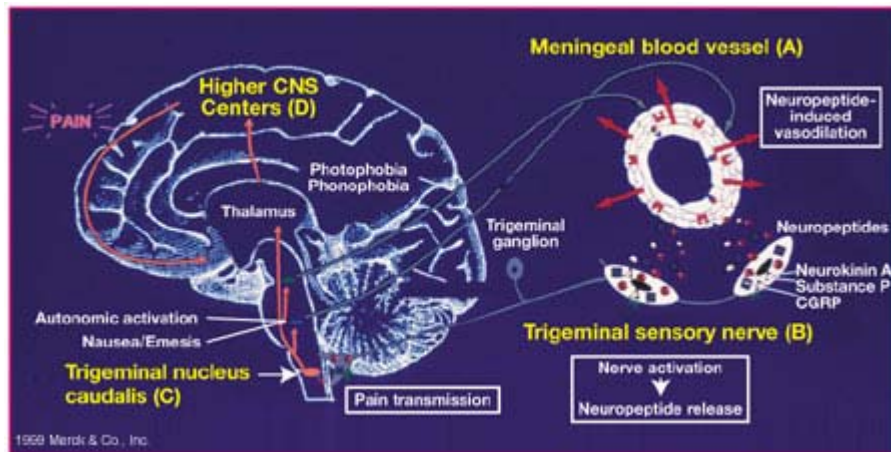


Figure 2.5 Trigeminovascular system activation and vasodilation [15].

2.3.5 The Serotonergic Abnormalities Hypothesis

The role of serotonin in migraine pathogenesis was taken into consideration after the discovery of the fluctuations in both plasma and platelet levels of serotonin during the migraine attack. The first substantial lead came in the early 1960s. Studies of migraine sufferers' urine revealed serotonin abnormalities. Additional research suggested that boosting serotonin levels could decrease symptoms [31].

The activation of platelets cause them to aggregate and release serotonin, thus the plasma levels of serotonin are increased. Increased level of serotonin is known to cause vasoconstriction whereas its decrease leads to vasodilation. During the attack plasma level of serotonin is observed to drop extremely. The large release of serotonin may be also seen from the increased serotonin levels in urine.

The serotonin abnormalities hypothesis explains migraine by an initial increase of plasma serotonin leading to vasoconstriction which may cause aura due to insufficient blood flow and later sharp decrease of serotonin levels leading to vasodilation. The mechanisms triggering the sudden changes remain uncertain according to the hypothesis. Moreover, unilateral nature of migraine could not be explained exactly by only the changes in serotonin levels [15].

In conclusion, the change in serotonin levels is proved to play an active but yet not clarified role in migraine pathophysiology by many researchers; such as Kovac et al. demonstrating the abnormal tendencies of migraineurs' platelets toward hyperaggregability and Lechner et al. observing greater degrees of platelet sensitivity to serotonin migraine patients, even during headache-free periods. What is known for sure is, it is impossible to claim that serotonin level abnormality is the main factor causing migraine [32, 33].

2.3.6 The Unifying Theory

The unifying theory attempts to combine the different approaches to migraine pathophysiology. According to the theory triggers such as hormonal levels, stress, certain chemicals, bright light or other factors stimulate specific centers in the brain. These centers include dorsal raphe nucleus and locus ceruleus which affects serotonin levels in brain and epinephrine levels, respectively. Blood flow reduction due to the functioning of the two centers may initiate cortical spreading depression. Although it is still commonly accepted that CSD stimulates trigeminal nerve, studies have shown that in addition to the CSD, some of the migraine triggers might also stimulate trigeminal nerve themselves. As described in neurovascular theory stimulation of trigeminal nerve leads to neurogenic inflammation and pain. As a result of the stimulation, vasodilation occurs in both the cerebral and extracranial vessels. The vasodilation in meningeal vessels redounds the pain.

Unlike other approaches, unifying theory proposes explanations for the symptoms of the prodrome and attack phases. Prodromal symptoms such as changes in appetite, food cravings, mood changes, yawning and drowsiness are associated to the disturbances in hypothalamus caused by the fibers emerging from dorsal raphe nucleus. Similarly, the difficulties in cognitive processes and control mechanism, migraineurs experience during attack, are attributed to the signals sent to the higher centers of the brain from the locus ceruleus [15].

3. IMAGING MIGRAINE

Causes of headaches, pain mechanisms and proving that the headache is “real”, have been very appealing topics to the scientists for decades. Despite the usage of the advanced imaging techniques, the conclusions are still controversial and explanations remain incomplete. Most of the time, structures in the brain were found to be perfectly normal, making it impossible to justify the symptoms observed by attributing them to the defective anatomy. Research in medicine is strictly dependent on the development of technology. Conventional imaging methods such as computed tomography (CT) and magnetic resonance imaging (MRI) only give information about the anatomy of the brain, which generally does not show any abnormalities in migraine. With the more sophisticated approaches to imaging, now functioning of the brain may be visualized complementary to its anatomy. Positron emission tomography (PET) is used to observe the regions of cell activation by measuring the change in blood flow. Another technique used for identifying brain activity is functional magnetic resonance imaging (fMRI). fMRI detects the active areas in brain, similar to PET, it tracks oxygen supply and blood flow, but by using the magnetic properties of hemoglobin to see whether it is combined with oxygen or not. These methods are used in numerous studies to learn more about which regions of the brain are active during certain activities, such as talking, calculating, memorizing or feeling pain [34].

3.1 Functional Near Infrared Spectroscopy (fNIRS)

Studies of the kinetics of cerebral metabolism and hemodynamics require fast, noninvasive and biochemically specific neuroimaging techniques. Near-infrared spectroscopy (NIRS) has the potential to measure directly neural activity via the optical “fast signal”, and also has the biochemical specificity necessary to measure hemodynamic changes, in terms of the concentrations of both oxy- and deoxyhemoglobin [35].

The main advantage of NIRS is based on the optical spectroscopic approach to measuring concentrations of oxyhemoglobin and deoxyhemoglobin in tissue. Biological tissue is relatively transparent to light in the near infrared band between 700 and 1000 nm.

The optical apparatus typically consists of light sources and detectors, which receives light after it has been transmitted through the tissue. The light source is coupled to the tissue via an optical fiber. Since light is highly scattered after entering tissue, another optical fiber bundle placed two to five cm away from the first one can collect light after it has passed through the tissue beneath the ends of the fibers (the optodes).

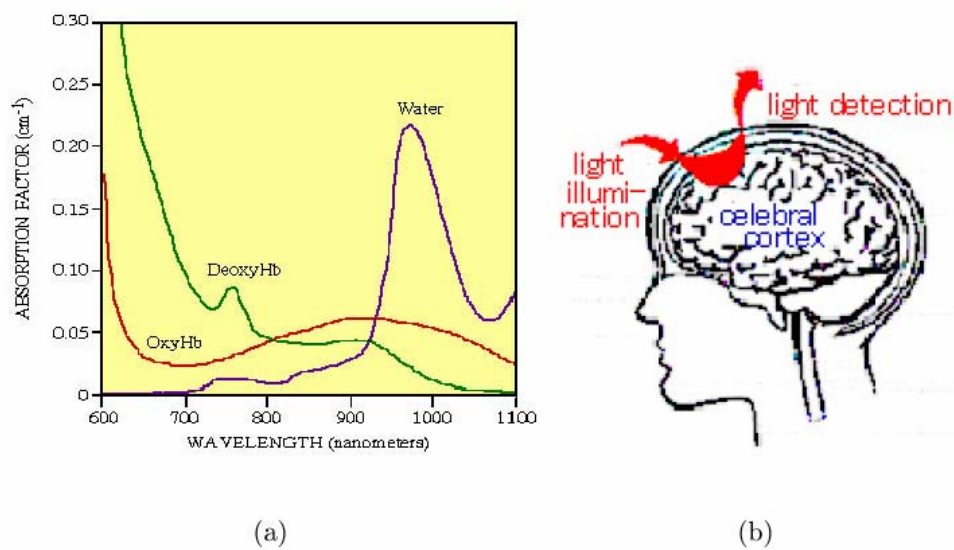


Figure 3.1 (a) The absorption spectrum of chromophores (b) the model of optical neuroimaging [36].

Low-intensity near infrared light entering tissue undergoes two major processes: absorption and scattering. The attenuation of light, due to absorption and scattering, can be expressed mathematically in an empirical modified Lambert-Beer law,

$$\ln(I_0 / I) = \mu \times d \times \sigma \quad (3.1)$$

where I_0 and I are the input and the output light intensities, respectively. μ is the medium absorption coefficient, d is the source-detector distance, and σ is the differential path length factor. A modified Lambert-Beer law indicates that the concentration and differential path length factor of a substance may be recovered from the light intensity measurements if, for example, the measurements are performed at several source-detector distances. Oxyhemoglobin (HbO_2) and deoxyhemoglobin (Hb) have characteristic absorption spectra in the visible and near infrared bands. Therefore, based on light

absorption measurements, concentration changes for these molecules can be measured [35, 37-39].

3.2 fNIRS in Cerebral Metabolism and Neurodynamics

In recent years many researchers have demonstrated that cerebral hemodynamic changes associated with functional brain activity can be assessed non-invasively in humans by near infrared spectroscopy. Hirth *et al.* used combined NIRS with transcranial Doppler sonography successfully, during a motor task and proved the feasibility of a simultaneous assessment of microcirculatory hemodynamics and cerebral oxygenation at high temporal resolution. [40]. Colier *et al.* exploited NIRS to assess human motor cortex oxygenation changes in response to cyclic coupled movements of hand and foot, and proved the detection of reproducible oxygenation patterns using single cycles of easy and difficult association tasks [41]. Motor cortex hemodynamics in human subjects under rest and motor stimulation condition was also studied by Toronov *et al.*, by using multichannel NIRS [42].

Apart from the motor activity studies, the visual and auditory stimulation have been investigated by NIRS. Kato *et al.* monitored human visual cortical function during photic stimulation with near infrared spectroscopy [43]. Cerebral oxygenation changes induced by auditory stimulation in newborns have been measured by Sakatani *et al.* using NIRS [44].

NIRS has also found uses in cognitive task studies, such as cognition activated low frequency modulation of light absorption in human brain by Chance *et al.* [45]. Villringer's study on NIRS as a tool for studying hemodynamic changes during activation of brain function in human adults showed that it's possible to detect cerebral concentrations of oxygenated and deoxygenated were assessed during cognitive tasks from frontal cortex as well during visual stimulation from the occipital lobe [39].

One of the early studies on migraine using NIRS is raised from the suspicion that the cortical spreading depression (CSD), the electrophysiological phenomenon which slowly moves over the cortex, may be a correlate of the neurological symptoms occurring

during migraine attack especially the migraine aura. In an animal study by Wolf, it has been shown that CSD is coupled to hemodynamic changes as well, an initial circumscribed hypoperfusion is followed by a hyperperfusion. Oxygenation changes associated with CSD induced hyperperfusion can be detected in animal experiments by means of near infrared spectroscopy [46].

4. METHOD

4.1 Experimental Protocol

Six subjects diagnosed with migraine without aura (four females, two males) according to IHS criteria and six healthy subjects (five males, one female) from the outpatient headache clinic, college students and hospital staff joined the study. Migraineurs were chosen to be free of any prophylactic medication and migraine attack at least three days prior to the experiment, including the experiment date. During the experiment the subjects were in supine position. For each subject, data collection started with 90 seconds of normal breathing period. Following the initial rest, subjects were asked to exhale the air and hold their breath at least 20 seconds. Regardless of time subjects could have hold their breath, at the end of the 30 second breath holding period, they were told to breath normally again. The resting time between breath holds was decided to be 90 seconds. This routine was repeated four times consecutively while the measurements were recorded. The experiment protocol is shown in Figure 4.1.

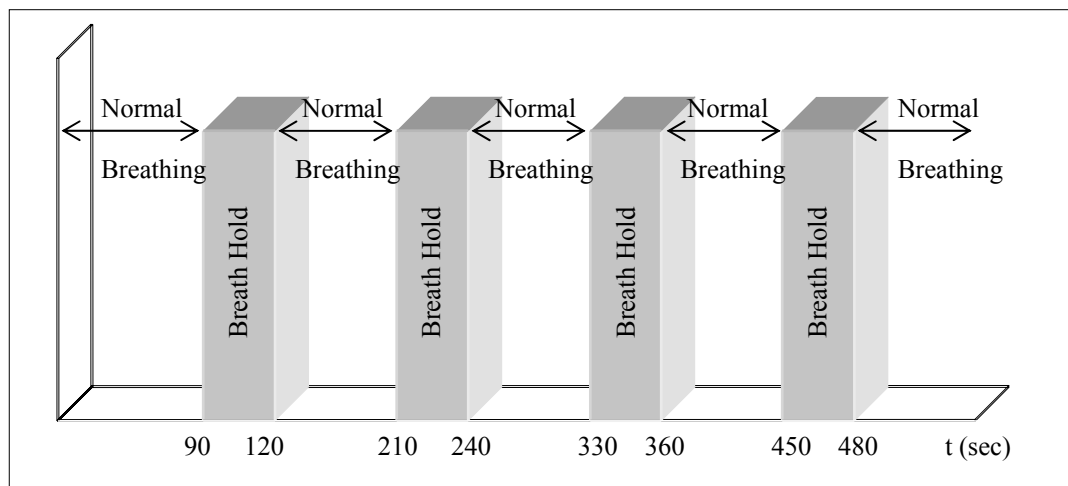


Figure 4.1 Breath holding protocol.

4.2 Data Collection

A fully reconfigurable fNIRS system developed at the Biophotonics Laboratory¹ (NIROXCOPE 201 in Figure 4.3) is used for obtaining data. The system is flexible physically for better fit and has higher number of detector pairs than the commercially available continuous wave systems.

The system has four light emitting diodes (Epitex, L4*730/4*805/4*850-40Q96-I) that are working in the near infrared spectrum as light sources and ten photodetectors (TI-Burr Brown, OPT101) which are sensitive in the NIR spectrum. The lights sources have multiple wavelengths including 730nm for *Hb* and 805nm for *HbO₂*. Four non-overlapping quadruples of photodetectors are obtained when time and wavelength are multiplexed. Detectors are placed equidistantly away from the source at the center within each quadrant. Detector layout is shown in Figure 4.2.

1	3	5	7	9	11	13	15
2	4	6	8	10	12	14	16

Figure 4.2 NIROXCOPE 201 probe spatial optode locations, optode number 1 being on the left top of the forehead.

The source detector distance is designed to be 2.5 cm, corresponding to 1.5 cm of average adult cortex depth making it possible to observe the first millimeters of the gray matter. For measurement, probe is placed on the forehead of the subjects aligning the base with the eyebrows and the middle with the Fz location from the EEG electrode placement. Flexible probe is adjusted on the subjects head with the band, without any covering material [47-49].

The data gathered from the experiment is used to calculate the relative changes in [*Hb*] and [*HbO₂*] signals according to the Beer Lambert Law. A sampling rate of 1.77 Hz is

¹ www.bme.boun.edu.tr/biophotonics

chosen corresponding to a time gaps of 565 msec between the sample points of both $[Hb]$ and $[HbO_2]$ signals [39].



Figure 4.3 A photograph of the functional optical imager, NIROSCOPE 201 [36].

4.3 Preprocessing Data

It is very probable that data gathered from the subjects includes noise, baseline drifts and other physiological phenomenon such as motion artifacts, breathing and arterial pulse. Eliminating this redundant information is fundamental in order to have reliable results.

The program developed in the MATLAB[®] environment is utilized for eliminating the spikes that are caused by the motion artifacts based on Pearson's study [50]. Outlier elimination is an important issue especially in studies like this involving nonlinear regression analysis, which will be mentioned again later. Furthermore, fluctuations in the heart rate due to respiration (periods typically in the couple of seconds range), blood pressure regulation (also called Meyer's waves with periods about 10 seconds) and arterial pulse is filtered out by a fourth degree Butterworth filter with a cut off frequency at 0.08 Hz. A moving average filter was used to eliminate the baseline drifts corresponding to high pass filtering at 0.03 Hz to remove the fluctuations due to heart rate [51-54].

4.4 Function Adaptation and Nonlinear Regression to [Hb] and [HbO₂] Signals

4.4.1 Gaussian Function

Gaussian function along with gamma function has been one of the most suitable and popular forms that have been chosen to represent BHR in fNIRS and fMRI studies. According to some researchers working in those fields, the Gaussian model accounts independently for the delay and dispersion of the hemodynamic responses and provides a more flexible and mathematically convenient model. When compared with Poisson and Gamma models, the ability of the Gaussian function to represent the hemodynamic responses of brain activation is found to be significantly better [55, 56].

However due to insufficient knowledge of the exact process of hemodynamic coupling, it is not possible to conclusively judge the excellence of a particular model. In order to choose the most efficient function to represent the response in this study, both gamma and gauss functions were considered. After running tests on sample data, gauss function exhibited superior accuracy at finding the parameters and fitting to experimental data.

BHR that we have obtained from the previous operations seem to be composed of three parts; an initial dip, a larger main response and finally an undershoot which may also interpreted as a recovery. To represent these three stages of the response accurately, summation of three different Gaussian functions was adopted to the model as in Eq. 4.1.

$$h(t) = A_1 e^{-\left[\frac{(t-D_1)}{\tau_1}\right]^2} + A_2 e^{-\left[\frac{(t-D_2)}{\tau_2}\right]^2} + A_3 e^{-\left[\frac{(t-D_3)}{\tau_3}\right]^2} \quad (4.1)$$

The equation above is the modified gaussian function that will be used in this study, for curve fitting and calculating the parameter values. The parameters A_1 , A_2 , and A_3 stand for the amplitudes, D_1 , D_2 and D_3 are the times where the function reaches the peak value,

τ_1 , τ_2 and τ_3 correspond to the dispersion which is proportional to the duration of the curve. Model can be seen in Figure 4.4.

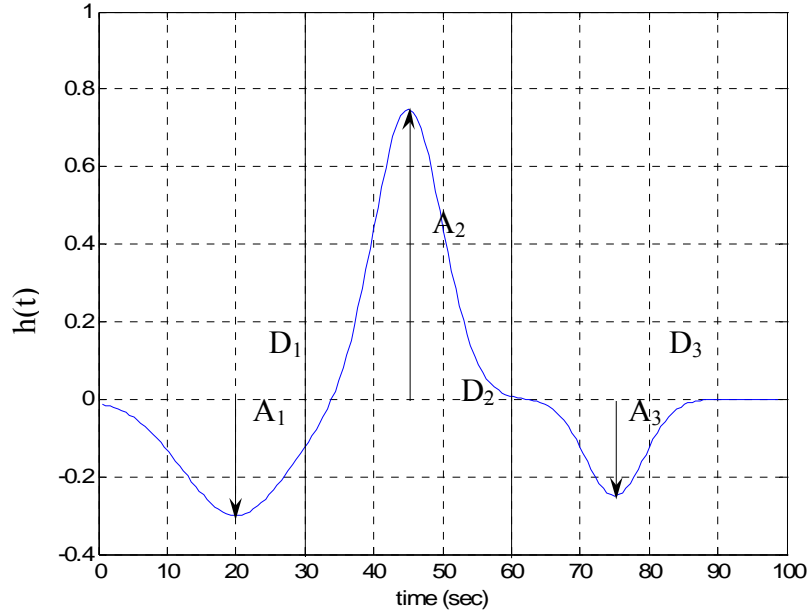


Figure 4.4 A representation of the brain hemodynamic response as the summation of three modified gaussian functions ($A_1 = -0.30$, $A_2 = 0.75$, $A_3 = -0.25$, $D_1 = 20$, $D_2 = 45$, $D_3 = 75$, $\tau_1 = 11$, $\tau_2 = 7$, $\tau_3 = 6$).

4.4.2 Nonlinear Regression

The basic idea of nonlinear regression is to relate a response Y to a vector of predictor variables $x = (x_1, \dots, x_k)^T$ just like linear regression. Nonlinear regression is characterized by the fact that the prediction equation depends nonlinearly on one or more unknown parameters. Whereas linear regression is often used for building a purely empirical model, nonlinear regression usually arises when there are physical reasons for believing that the relationship between the response and the predictors follows a particular functional form. A nonlinear regression model has the form

$$Y_i = f(x_i, \theta) + \varepsilon_i, \quad i = 1, \dots, n \quad (4.2)$$

where the Y_i are the responses, f is a predefined function, the modified gaussian function in this study, of the covariate vector $x = (x_1, \dots, x_k)^T$ and the parameter vector $\theta = (\theta_1, \dots, \theta_p)^T$

and ε_i are random errors. The ε_i are usually assumed to be uncorrelated with zero mean and constant variance.

The unknown parameter vector θ in the nonlinear regression model is estimated from the data by minimizing a suitable goodness-of-fit expression with respect to θ . The most popular criterion is the sum of squared residuals,

$$\sum_{i=1}^n [y_i - f(x_i, \theta)]^2 \quad (4.3)$$

and the estimation based on this criterion is known as nonlinear least squares. If the errors ε_i follow a normal distribution, then the least squares estimator for θ is also the maximum likelihood estimator. Except in a few isolated cases, nonlinear regression estimates must be computed by iteration using optimization methods to minimize the goodness-of-fit expression [57].

One of the biggest advantages of nonlinear regression over many other techniques is its compatibility with the broad range of functions. Although simpler regression methods may be preferred for linear cases, most of the scientific and engineering problems turn out to be inherently nonlinear. Another advantage of nonlinear regression is the efficient use of data and producing good estimates of parameters with relatively small sets of data. In addition to these, nonlinear regression also provides a fairly well-developed theory for computing confidence, prediction and calibration intervals to answer scientific and engineering questions. Although in most cases they are only approximately correct, they generally work quite well in practice.

In spite of its sophisticated approach, nonlinear regression has some flaws which may cause in inaccurate results, if they are not paid attention to. The major problem with the nonlinear regression is the fact that it uses iterative optimization procedures to compute the parameter estimates. Unlike linear regression, the least squares estimates of the parameters cannot be obtained analytically and iterative procedures require the user to provide initial values for the unknown parameters before optimization. The starting values must be reasonably close to the as yet unknown parameter estimates or the optimization

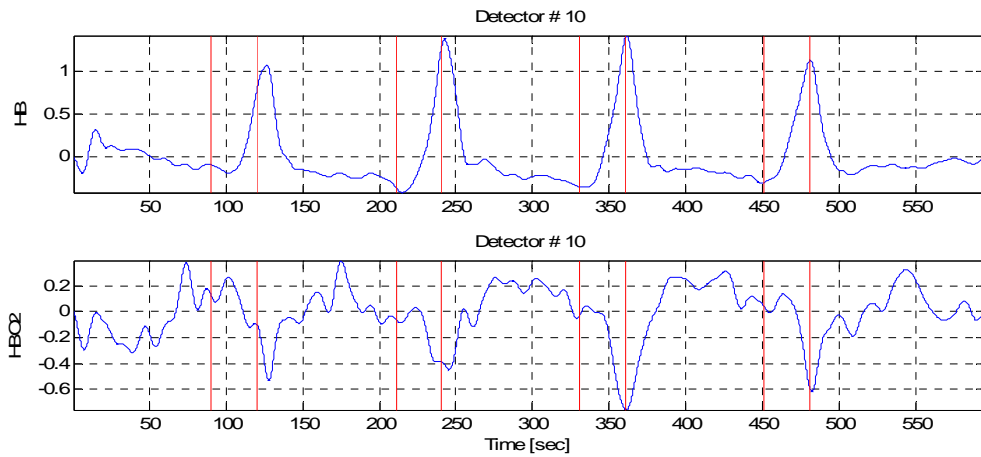
procedure may not converge. A local minimum may be converged rather than the global minimum that defines the least squares estimates, if the initial values are not appropriate. Another disadvantage of nonlinear regression is the strong sensitivity to outliers. Just as in a linear least squares analysis, the presence of a few outliers in the data can seriously affect the results of a nonlinear analysis [58].

4.5 Data Processing and Curve Fitting

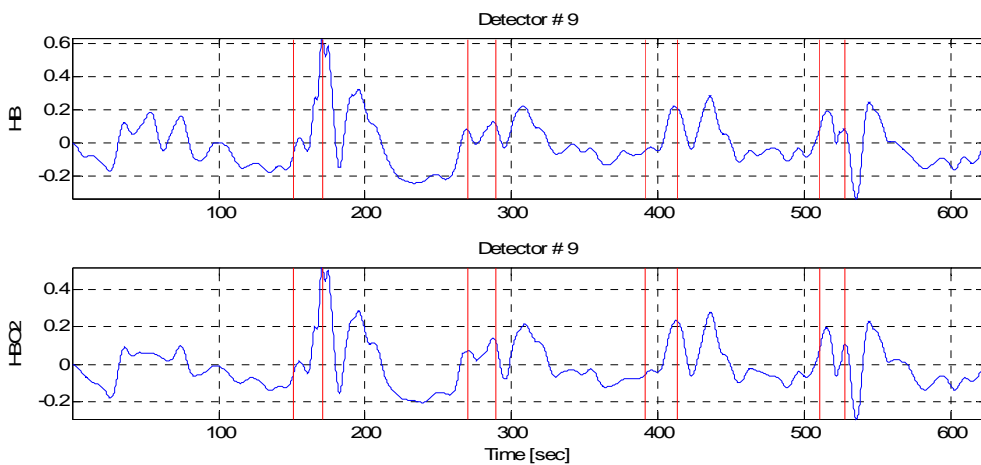
As a result of the preprocessing procedure, for each one of the 12 subjects, we obtained $[Hb]$ and $[HbO_2]$ data separately from 16 detectors. Each detector recording lasts about 540 seconds starting with a 90 second initial rest, followed by four breath holding episodes. The breath holding episodes are 30 seconds long and separated by resting periods of 90 seconds. A function working in collaboration with the preprocessing program is coded in MATLAB[®] environment, in order to organize the data in a form that will be useful for further analysis and comparison. First task of the program is averaging the data from the 16 detectors for each subject. After calculating and recording the averaged signal, the breath holding sequences are detected and a window of 100 seconds, beginning 30 seconds before the and ending 40 seconds after breath holding sequence is taken for each four of the breath holds. That window allows us to observe the three responses, namely initial dip, main response and the recovery, without interfering with the neighboring breath hold. Output of the function is a matrix holding eight 100 seconds long signals, corresponding to first, second, third and fourth breath holds for each subject, in terms of $[Hb]$ and $[HbO_2]$. After that point, a second function exploiting MATLAB[®] function *lsqcurvefit*, which aims to solve nonlinear least squares problems, is created and run on the data.

The second function created, fits three different Gaussian functions to $[Hb]$ and $[HbO_2]$ signals as stated in previous sections. The nonlinear regression analysis performed on each breath hold data provides nine parameters, three parameters for each one of initial dip (first gaussian function), main response (second gaussian function) and recovery (third gaussian function) phases. Three parameters that belong to the modified gaussian function are amplitude, time to peak and dispersion, represented by A , D and τ respectively. Final

task of the function is to plot the actual data and the curve formed by the parameters obtained by regression, for visual presentation of the fit (Figure 4.6).

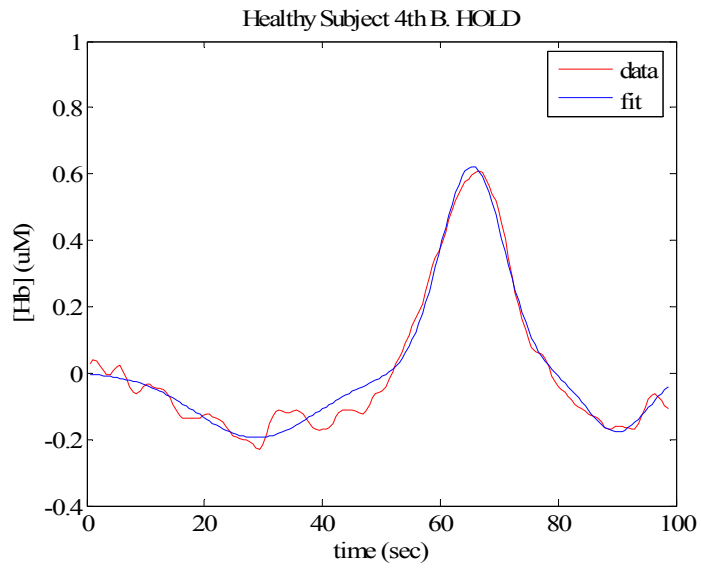


(a)

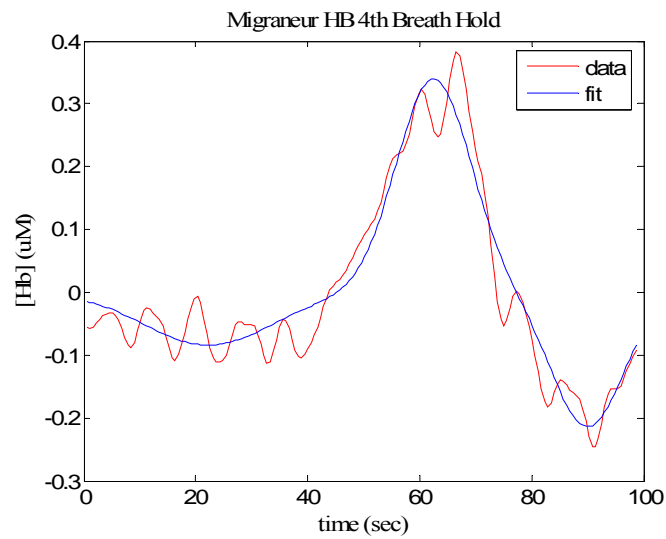


(b)

Figure 4.5 Preprocessed $[Hb]$ and $[HbO_2]$ data during breath hold experiment for (a) a healthy subject and (b) a migraineur (Vertical lines indicate the beginning and end of the breath holding and true values for Hb and HbO_2 data are in μM).



(a)



(b)

Figure 4.6 Actual [Hb] data and its nonlinear regression curve fit from a (a) healthy subject and a (b) migraine patient (The smooth lines are the fit to real data).

5. RESULTS AND DISCUSSION

The parameters obtained from the nonlinear regression exhibits significant differences for both Hb and HbO_2 dynamics. Although differences of dispersion (τ) values are not crucial, according to the statistical test, ANOVA, both amplitudes (A) and time to peak (D) values of the healthy subjects and migraineurs are found to be quite representative of the group they belong.

One way ANOVA test performs a comparison test for two or more groups of data in terms of their similarity and returns a p value to indicate the degree of similarity. In our case, parameters for migraineurs and healthy subjects having p values less than 0.05 are accepted to be potential candidates for diagnostic criteria, reciprocating to a reliance interval of 95per cent. Examples of the ANOVA analysis on some chosen parameters are shown in Figure 5.1. As can be seen from the figure, smaller p values indicate more separate intervals of parameter values for healthy subjects and migraineurs.

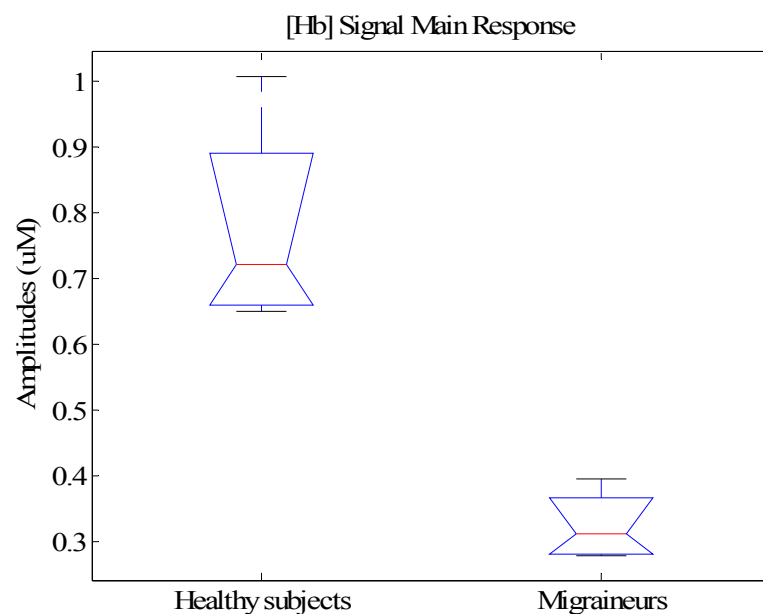
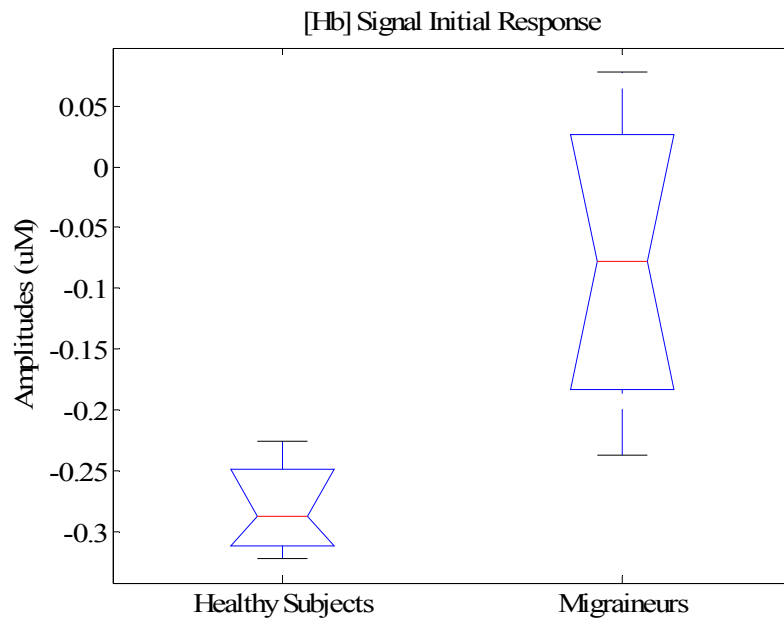
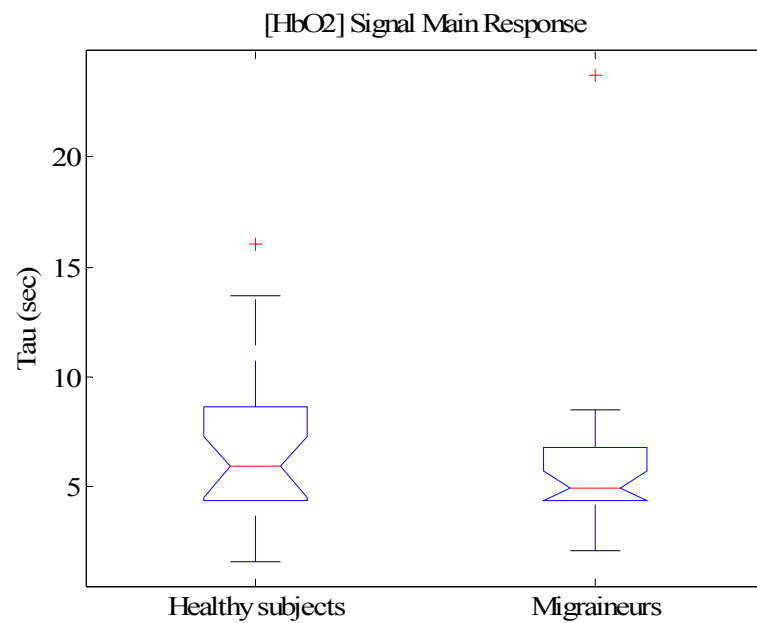


Figure 5.1 Statistically significant data with $p= 0.002$, according to ANOVA analysis.



(a)



(b)

Figure 5.2 Examples for ANOVA analysis with 2 different data sets; first one being statistically significant with (a) $p=0.0291$ and the other having no diagnostic value (b) $p=0.5878$.

In order to present a visual reference for the results that will be discussed in the following sections, modeled Hb and HbO_2 dynamics are plotted in Figure 5.5 and 5.6, respectively. The estimated values for the parameters are used with the modified gaussian function to form the response models.

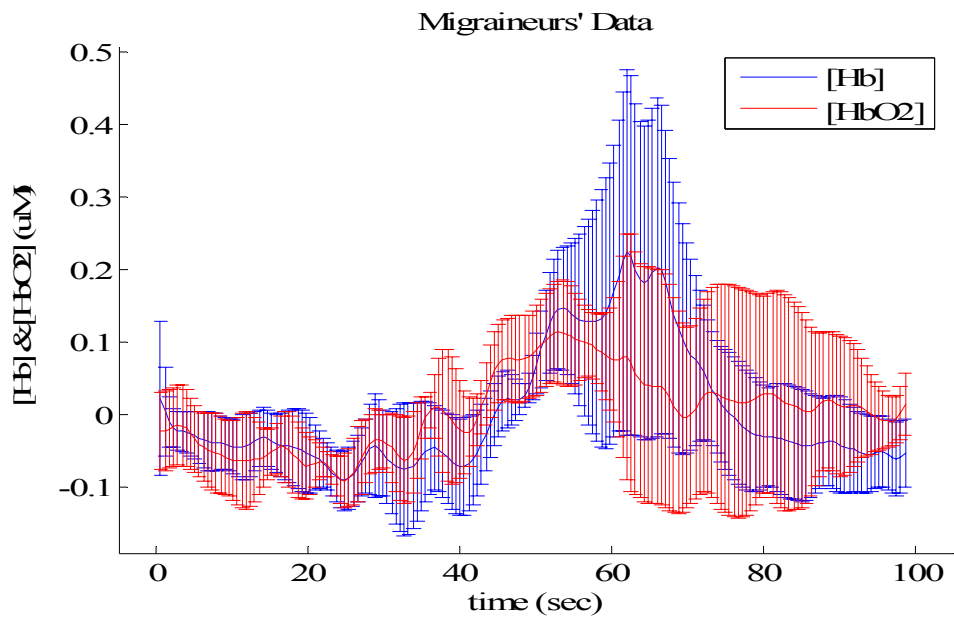
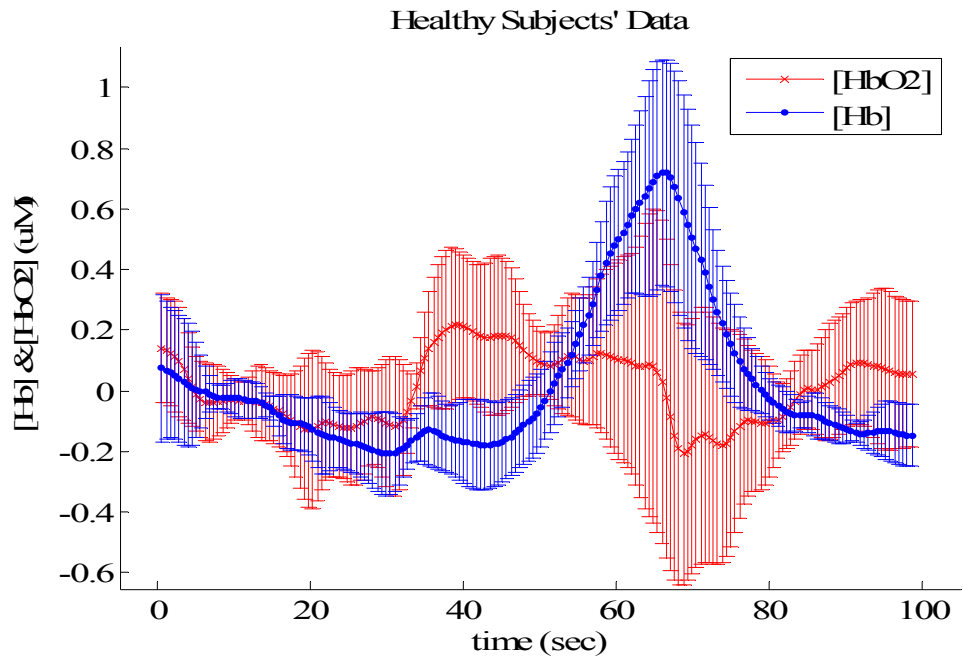
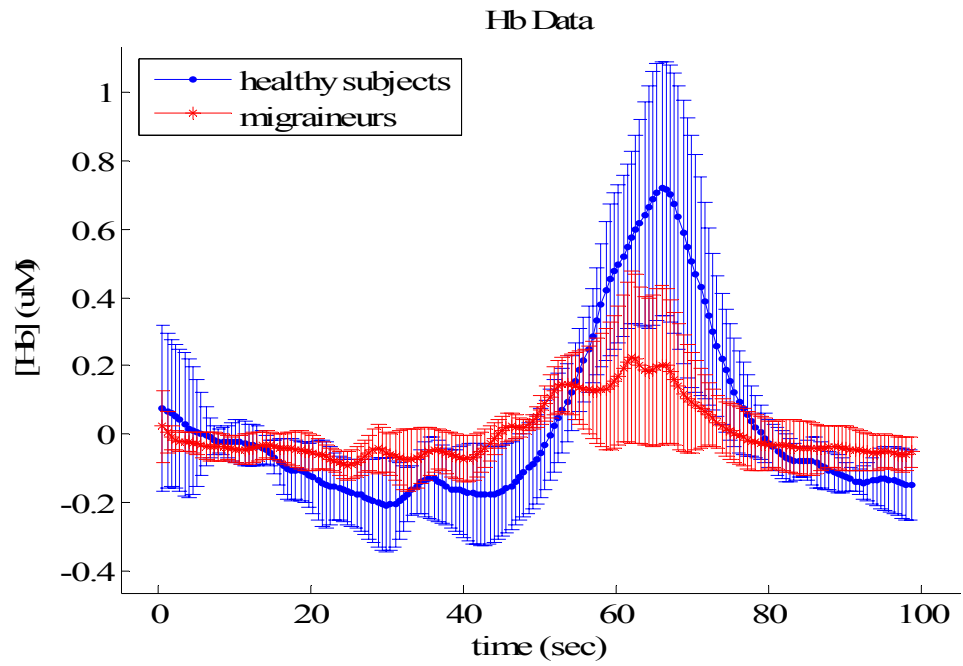
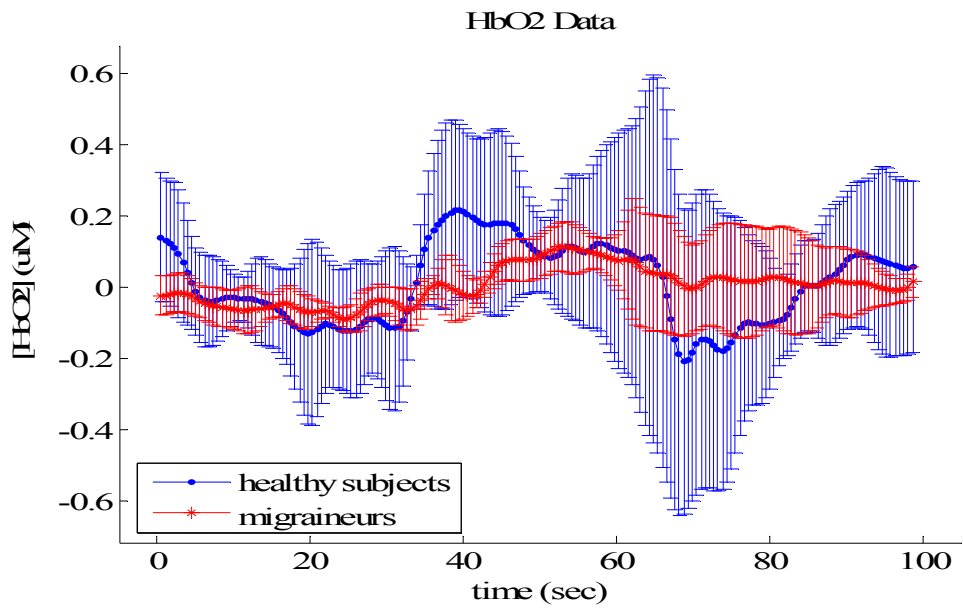


Figure 5.3 Real Hb and HbO₂ data with standard deviations obtained for (a) healthy subjects and (b) migraineurs with mean values shown as the lines passing through error bars.



(a)



(b)

Figure 5.4 Real data with standard deviations obtained from healthy subjects and migraineurs (a) [Hb] (b) [HbO₂] with mean values shown as the lines passing through error bars.

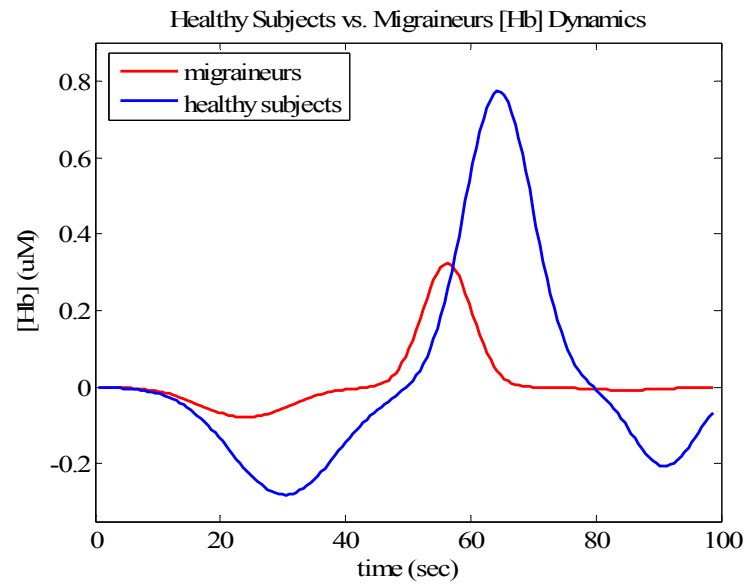


Figure 5.5 Constructed [Hb] dynamics using the estimated parameters for healthy subjects and migraineurs in comparison.

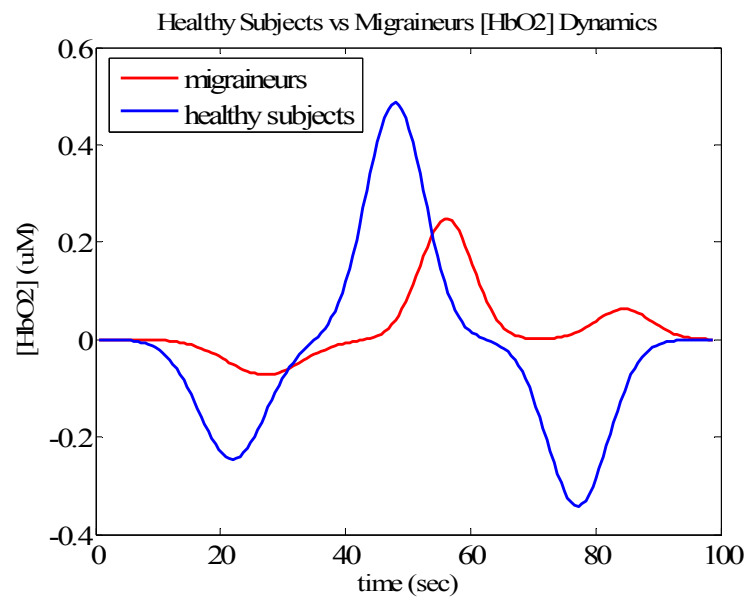


Figure 5.6 Constructed [HbO₂] dynamics using the estimated parameters for healthy subjects and migraineurs in comparison.

5.1 Amplitude (A)

While analyzing the results for the amplitude, the ability of the vascular dynamics to adapt to breath holding procedure was an additional point of interest. In order to see whether there is a difference between vascular systems of migraineurs and healthy subjects

in terms of “learning” how to hold their breath, four breath holds were both observed separately and in groups of four, for each parameter.

5.1.1 [Hb] Signal Amplitudes

Once the parameters regarding the *Hb* dynamics are obtained, the first point to draw one’s attention is the differences in the magnitude of the amplitudes for migraine patients and normal subjects. Amplitudes of the initial and main gaussians for migraineurs are equal to less than half of those for healthy subjects and one fourth for the recovery response. These results may be attributed to the vasoconstrictive nature of the patients’ cerebral vessels, which may be suppressing the response a healthy cerebrovascular system will generate. P-analysis test also proves that amplitude values, for all responses, are significantly different for the members of the two groups.

Table 5.1
Amplitude (A) values of averaged [Hb] signal for four breath holds (mean \pm std).

Phase	Healthy Subjects	Migraineurs	p (subjects)
Initial	-0.28 \pm 0.12	-0.10 \pm 0.06	0.009**
Main	0.77 \pm 0.38	0.37 \pm 0.27	0.047*
Recovery	-0.21 \pm 0.05	-0.05 \pm 0.09	0.005**

* p < 0.05, ** p < 0.01 statistically significant data

The amplitude values were grouped among the initial, main and recovery responses by using the mean values of first, second, third and fourth breath holds of the subjects. This analysis may give insight about the amplitude differences and limits of each response for healthy subjects and migraineurs. The intervals were also found to be distinctive according to ANOVA test (Table 5.2).

Investigating the consecutive breath holds further, in terms of the amplitude changes (Table 5.3 and 5.4) ended up in interesting results. It is observed that for healthy subjects, both the amplitude and the percentage changes between the breath holds of the main response tend to converge exponentially to a stable value. On the contrary,

percentage changes and amplitudes of the main response for the migraineurs fluctuate indecisively.

Table 5.2

Amplitude (A) values of $[Hb]$ signal for groups of the mean values of the four breath holds (mean \pm std).

Phase	Healthy Subjects	Migraineurs	p (breath holds)
Initial	-0.28 ± 0.04	-0.10 ± 0.07	0.029*
Main	0.77 ± 0.16	0.37 ± 0.07	0.002*
Recovery	-0.21 ± 0.05	-0.05 ± 0.03	0.003*

* $p < 0.05$, statistically significant data

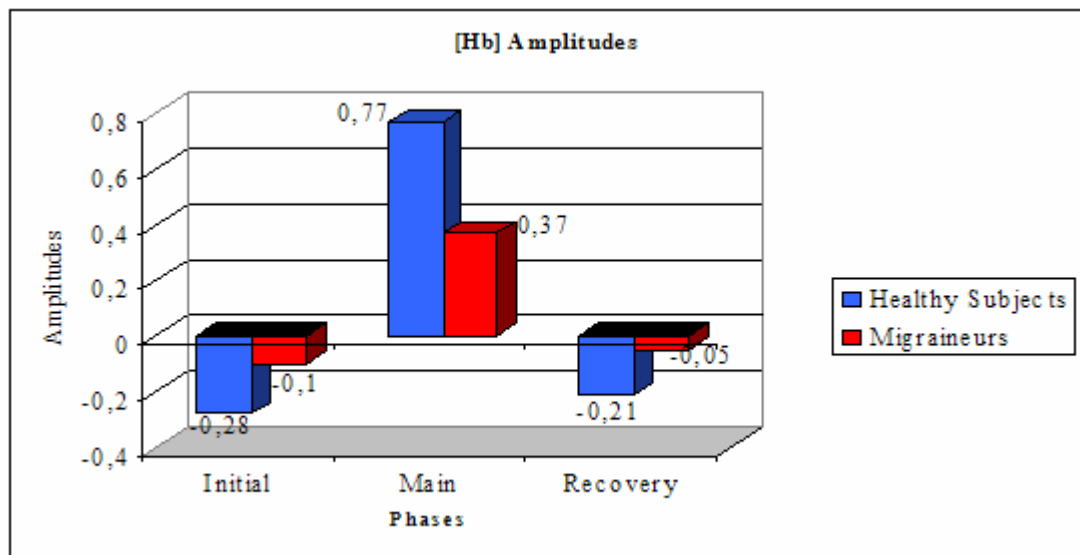


Figure 5.7 Mean amplitude (A) values of $[Hb]$ signal of healthy subjects and migraineurs in μM .

On the other hand, when breath hold episodes are compared one by one among healthy subjects and migraineurs, the findings were not as satisfying as they were when they are grouped. The reason for that is, unlike healthy subjects' amplitude values, migraineurs parameters fluctuate randomly either decreasing or increasing without following a certain detected pattern, with the exception of initial dip amplitude which remains quite stable for all breath holds.

The results so far are consistent with the hypothesized inherent vasomotor instability by some researchers as mentioned by Campbell *et al.* [22].

Table 5.3
Amplitude (A) values of [Hb] signal for consecutive breath holds (mean \pm std).

		Breath Hold			
Phase	Subjects	1st	2nd	3rd	4th
Initial	Healthy S.	-0.32 \pm 0.29	-0.30 \pm 0.18	-0.27 \pm 0.11	-0.23 \pm 0.05
	Migraineur	-0.10 \pm 0.08	-0.10 \pm 0.09	-0.10 \pm 0.07	-0.10 \pm 0.07
	p	0.10	0.03	0.01	0.01
Main	Healthy S.	1.00 \pm 0.77	0.77 \pm 0.46	0.67 \pm 0.34	0.65 \pm 0.27
	Migraineur	0.28 \pm 0.19	0.45 \pm 0.33	0.44 \pm 0.54	0.32 \pm 0.23
	p	0.05	0.29	0.28	0.05
Recovery	Healthy S.	-0.24 \pm 0.12	-0.25 \pm 0.12	-0.13 \pm 0.18	-0.21 \pm 0.14
	Migraineur	-0.01 \pm 0.14	-0.05 \pm 0.11	-0.08 \pm 0.16	-0.08 \pm 0.09
	p	0.01	0.01	0.67	0.08

Table 5.4
Percentage changes between breath holds in [Hb] amplitude (A).

Subjects	Phase	1st Change	2nd Change	3rd Change
Healthy Subjects	Initial	6.22	9.46	17.57
	Main	23.30	13.59	2.68
	Recovery	5.44	49.70	67.64
Migraineurs	Initial	6.71	6.54	1.54
	Main	60.3191	2.2577	60.31
	Recovery	347.14	76.05	7.23

5.1.2 [HbO_2] Signal Amplitudes

Unlike the results obtained from Hb signal, mean values of the main response amplitude in migraineurs' data is found to be quite stable from the first breath hold to the fourth one, mimicking the main response amplitude of the healthy subjects; but just as in the Hb case, the amplitudes are very close to the half of the amplitudes of the healthy subjects'. However the differences in the amplitudes of initial and recovery phases are more striking for the two groups (Table 5.5 and Table 5.6). Surprisingly, most of the migraine patients tend to develop positive recovery response amplitudes, although some of

their breath hold episodes provide negative amplitude values too. Statistically testing the data showed that the only reliable one among the three amplitudes to decide whether a subject is a migraineur or not according to the model developed, is the recovery response amplitude (Table 5.5). However, if the mean values regarding each breath hold (i.e. first, second, third and fourth breath holds) are used to form groups for all three phases, a different view is captured. The values obtained are quite different from each other for the subject sets, and the results of the p-analysis test are affirmative, providing at least more insight about the differences in the HbO_2 dynamics.

Table 5.5

Amplitude (A) values of averaged $[HbO_2]$ signal for four breath holds (mean \pm std).

Phase	Healthy Subjects	Migraineurs	p (subjects)
Initial	-0.25 ± 0.32	-0.07 ± 0.06	NS
Main	0.49 ± 0.29	0.25 ± 0.15	NS
Recovery	-0.34 ± 0.36	0.06 ± 0.20	0.04*

* $p < 0.05$: statistically significant data, NS: Not Significant

Table 5.6

Amplitude (A) values of $[HbO_2]$ signal for groups of the mean values of the four breath holds (mean \pm std).

Phase	Healthy Subjects	Migraineurs	p (breath holds)
Initial	-0.25 ± 0.08	-0.07 ± 0.06	0.0183**
Main	0.49 ± 0.04	0.25 ± 0.01	6.0094e-005**
Recovery	-0.34 ± 0.16	0.06 ± 0.05	0.0031*

* $p < 0.05$, ** $p < 0.02$, statistically significant data

The amplitude parameters which appertain each the breath holding sequences are examined one by one, due to the reasons mentioned in the section 5.1. As stated above the individual amplitude parameters of breath holds are found to be insignificant on diagnostic basis. However, the percentage changes of the amplitudes seem to follow some patterns. Both of the main response amplitudes fluctuate with relatively small percentage values, the migraineurs' response being more suppressed. Percentage changes for initial dip and recovery phases gradually decrease with every breath hold for healthy subjects.

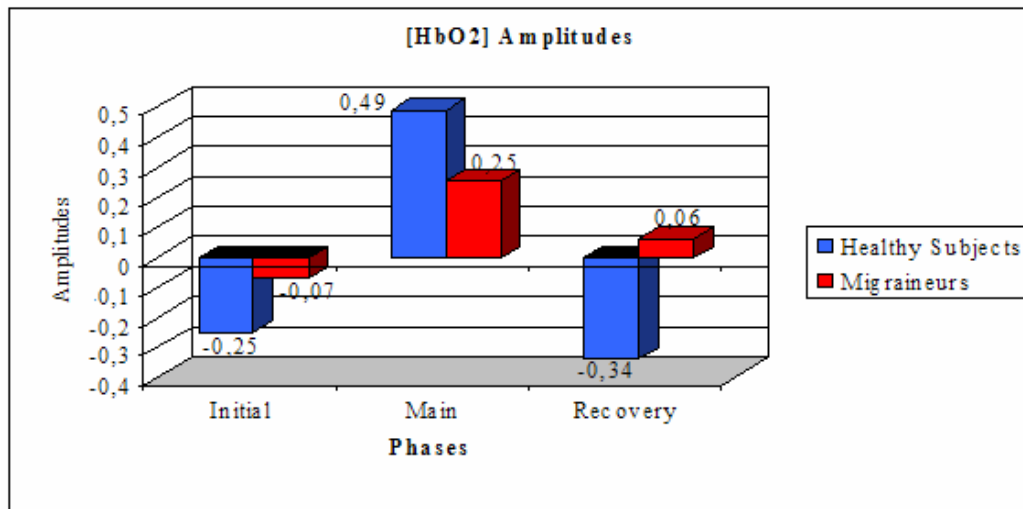


Figure 5.8 Mean amplitude (A) values of $[HbO_2]$ signal of healthy subjects and migraineurs in μM .

Table 5.7
Amplitude (A) values of $[HbO_2]$ signal for consecutive breath holds (mean \pm std).

Phase	Subjects	Breath Hold			
		1 st	2 nd	3 rd	4 th
Initial	Healthy S.	-0.18 ± 0.43	-0.36 ± 0.44	-0.26 ± 0.21	-0.18 ± 0.40
	Migraineur	0.01 ± 0.14	-0.15 ± 0.06	-0.09 ± 0.15	-0.07 ± 0.14
	p	0.33	0.25	0.13	0.52
Main	Healthy S.	0.54 ± 0.35	0.49 ± 0.32	0.43 ± 0.36	0.48 ± 0.36
	Migraineur	0.24 ± 0.14	0.24 ± 0.22	0.25 ± 0.17	0.26 ± 0.16
	p	0.08	0.14	0.31	0.20
Recovery	Healthy S.	-0.15 ± 0.53	-0.54 ± 0.67	-0.38 ± 0.25	-0.30 ± 0.32
	Migraineur	0.14 ± 0.24	0.04 ± 0.21	0.05 ± 0.22	0.03 ± 0.23
	p	0.25	0.07	0.01	0.07

For the same parameters, migraineurs' case is quite different, the amplitudes of the four breath hold episodes do not only decrease or increase irregularly but they also tend to have both positive and negative values in a four breath hold sequence as shown in Table 5.7. These characteristics of migraineous response might be evaluated as another clue about migraineurs having a possible inherent incapability for cerebral autoregulation.

The second distinguishing parameter of the model is time to peak (D) whose difference for healthy subjects and migraineurs might be detected even visually from

Figures 5.5 and 5.6. Because of the observed relation between time to peak values of the Hb and HbO_2 signals, the results will be discussed together.

Table 5.8
Percentage changes between breath holds in $[HbO_2]$ amplitude (A).

Subjects	Phase	1 st Change	2 nd Change	3 rd Change
Healthy Subjects	Initial	102.49	30.28	29.27
	Main	8.91	13.30	12.46
	Recovery	255.92	30.01	19.10
Migraineurs	Initial	2.10	0.04	0.02
	Main	1.58	5.87	3.81
	Recovery	74.80	39.59	54.09

5.2 Time to Peak (D)

Healthy subjects have higher time to peak values than migraineurs when the $[Hb]$ signal is concerned, but their peak points are found to be smaller for the $[HbO_2]$ response (Table 5.9).

Normally in a healthy person it is expected that $[HbO_2]$ will increase due to the blood flow increase to reduce hypercapnic effect till the middle of the hold episode. $[Hb]$ will start to climb to its peak value, where $[HbO_2]$ starts to decrease from its maximum. But that may not be the case in migraine patients. Because of the vasoconstriction in cerebral blood vessels when migraineurs hold their breath, blood flow cannot increase as much as it can in healthy subjects. Blood flow will be slower due to vasoconstrictive nature of the vessels and stored oxygen will be enough to continue increasing $[HbO_2]$ for a longer time than it will be for healthy people, but the increase will be at a slower rate and reach a lower amplitude than normal response does; just as what we observed. Moreover, it is understandable for $[Hb]$ signal to reach peak values for migraineurs earlier than healthy people; because oxygen supply is not backing up the oxygen consumption fast enough, in a way loading more $[Hb]$ as input to the system, leading to an even earlier response in $[Hb]$ dynamics which is already triggered by breath hold (Figure 5.9).

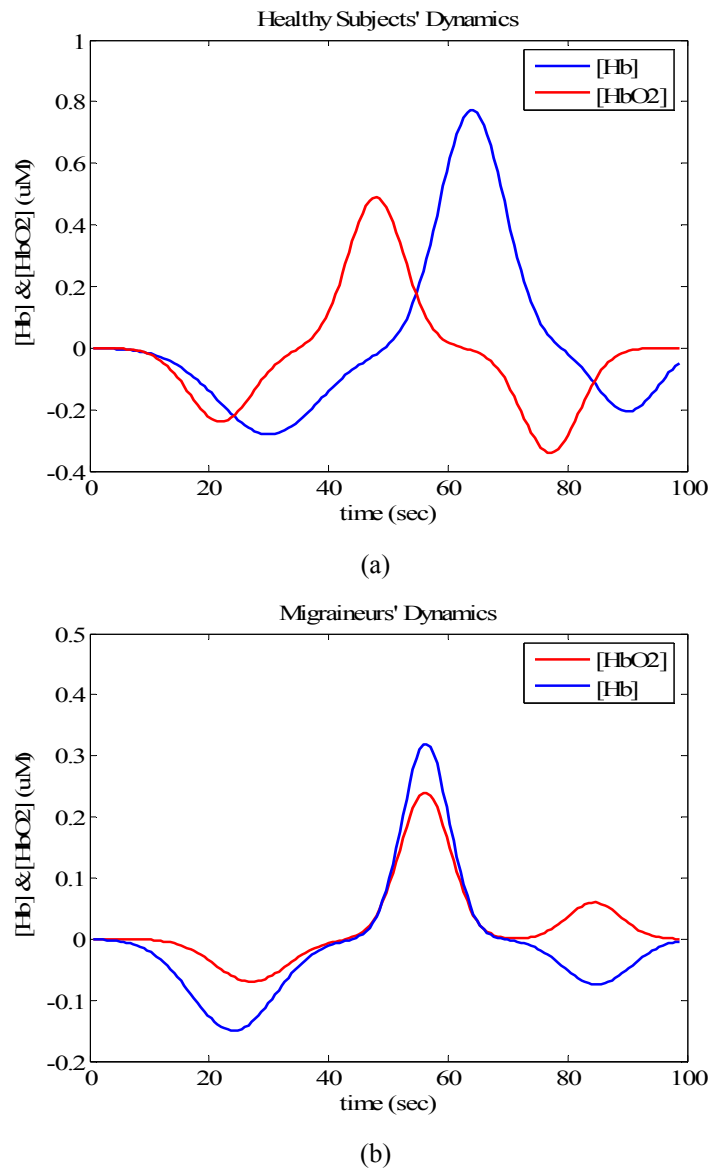


Figure 5.9 Estimated $[Hb]$ and $[HbO_2]$ dynamics of (a) healthy subjects and (b) migraineurs.

Table 5.9
Time to peak (D) values of averaged signals for four breath holds (mean \pm std).

	Phase	Healthy Subjects	Migraineurs	p
$[Hb]$	Initial	30.25 ± 8.59	24.02 ± 5.83	0.0052**
	Main	64.44 ± 3.27	56.24 ± 8.14	$3.5721e-005^{**}$
	Recovery	90.99 ± 6.62	84.88 ± 8.39	0.0074**
$[HbO_2]$	Initial	21.92 ± 7.50	27.08 ± 7.68	0.0228*
	Main	47.92 ± 10.35	56.14 ± 7.63	0.0030**
	Recovery	77.09 ± 9.02	84.45 ± 6.65	0.0024**

* $p < 0.05$, ** $p < 0.01$, statistically significant data

5.3 Dispersion (τ)

The dispersion parameter which is proportional to the duration of the gaussian model fitted to each phase is the third parameter investigated. However no significant differences or characteristics of the dispersions have been detected during the analysis. That result is confirmed by running the ANOVA test on data as shown in Table 5.10.

Table 5.10
Dispersion (τ) values of averaged signals for four breath holds (mean \pm std).

	Phase	Healthy Subjects	Migraineurs	p
[Hb]	Initial	12.00 \pm 5.38	9.93 \pm 4.55	NS
	Main	7.73 \pm 2.16	5.63 \pm 2.75	NS
	Recovery	7.21 \pm 2.04	7.95 \pm 4.99	NS
[HbO₂]	Initial	7.54 \pm 4.18	8.49 \pm 4.53	NS
	Main	6.65 \pm 3.54	6.05 \pm 4.09	NS
	Recovery	6.91 \pm 4.41	6.26 \pm 3.25	NS

NS: not significant

6. CONCLUSIONS

In this study, it was intended to observe the cerebrovascular dynamics of migraineurs by using fNIRS. The characteristics of healthy and migraineous response and the possibility of using cerebrovascular dynamics as a migraine indicator were the main topics of interest.

The model and method applied have been quite successful for representing the hemodynamic responses of subjects with and without migraine. The analysis and comparison of the model parameters of both groups have shown that their cerebrovascular dynamics exhibit significant differences. Compared to healthy subjects, migraineurs' responses were suppressed and mostly unpredictable. The diversities observed were attributed to the inherent instability of migraineurs' vasomotor responses as proposed by some other researchers.

6.1 Recommendations for Future Work

The subjects who participated to this study confirmed that they held their breath at least 20 seconds as they were asked. However, measuring the airflow through the mouth and nose or monitoring breathing by placing elastic belts around chest and abdomen might be a more reliable way to obtain the beginning and end of the breath holding periods. Knowledge of the exact duration of the breath holds might allow us to interpret the model parameters more accurately. Especially the third parameter, dispersion (τ), which is proportional with the duration of the curve and does not seem to exhibit significant deviations between migraineurs and healthy subjects, might carry information if the breath holding durations are found to be significantly different for the two groups.

APPENDIX A

SCATTER GRAPHICS

This section includes the graphics of the additional analysis on the relationship between the model parameters amplitude (A) and time to peak (D) for the subjects with and without migraine. Scatter graphics for the three responses, namely initial, main and recovery, are obtained for each one of Hb and HbO₂ signals. Each breath hold is represented with a different marker to make following the movements of the points along the breath holding sequences easier, and the markers are color coded; red for migraineurs and blue for healthy subjects (Figure A.1, Figure A.2, Figure A.3 and Figure A.4). But the scatter points did not always converge to certain values for healthy subjects as they were converging for amplitude and time to peak parameters individually.

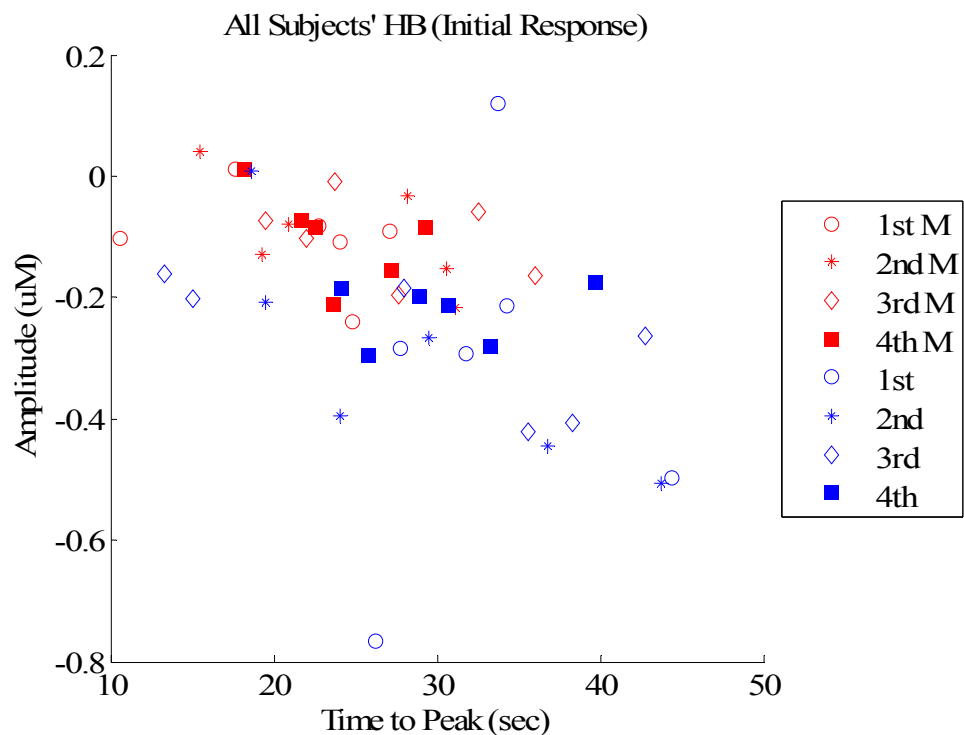
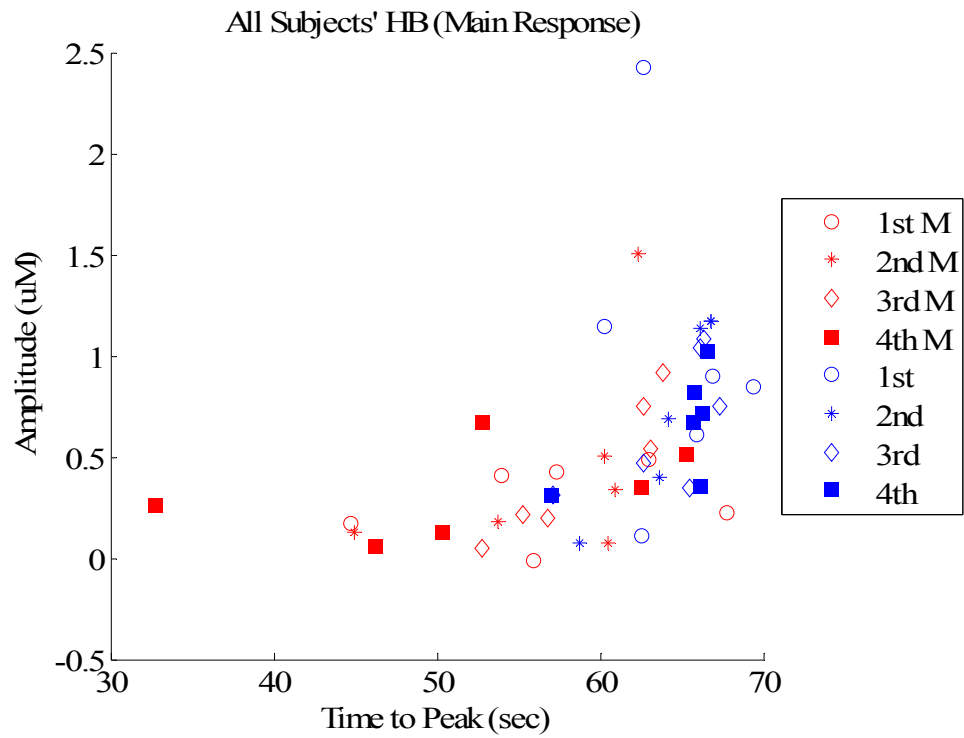
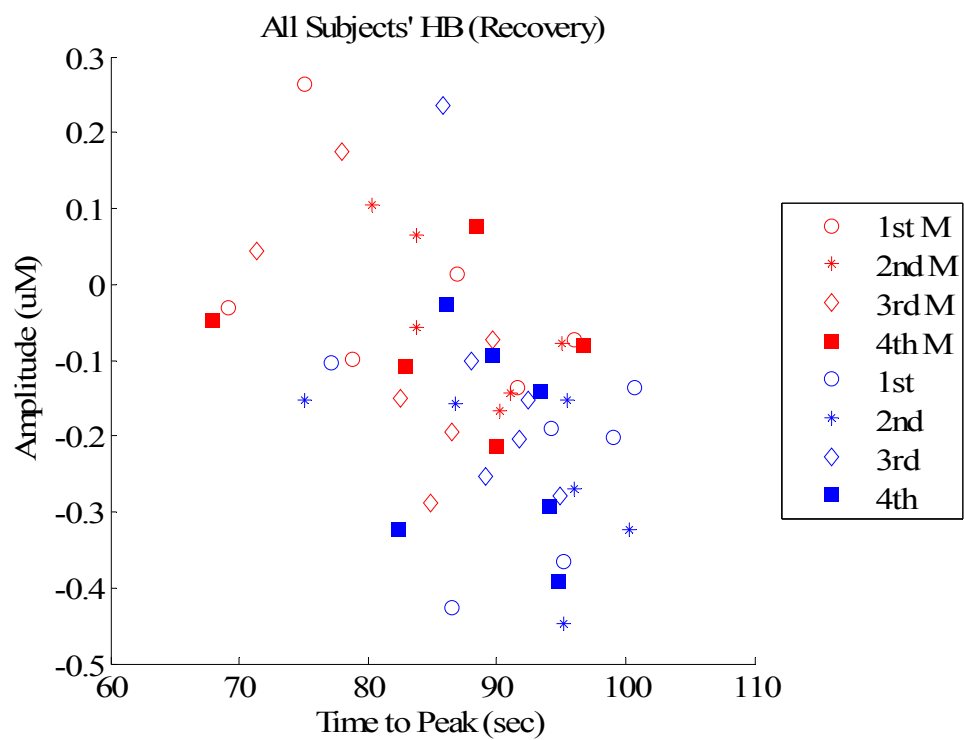


Figure A.1 [Hb] signal initial response scatter graphics for four consecutive breath holds from all subjects.

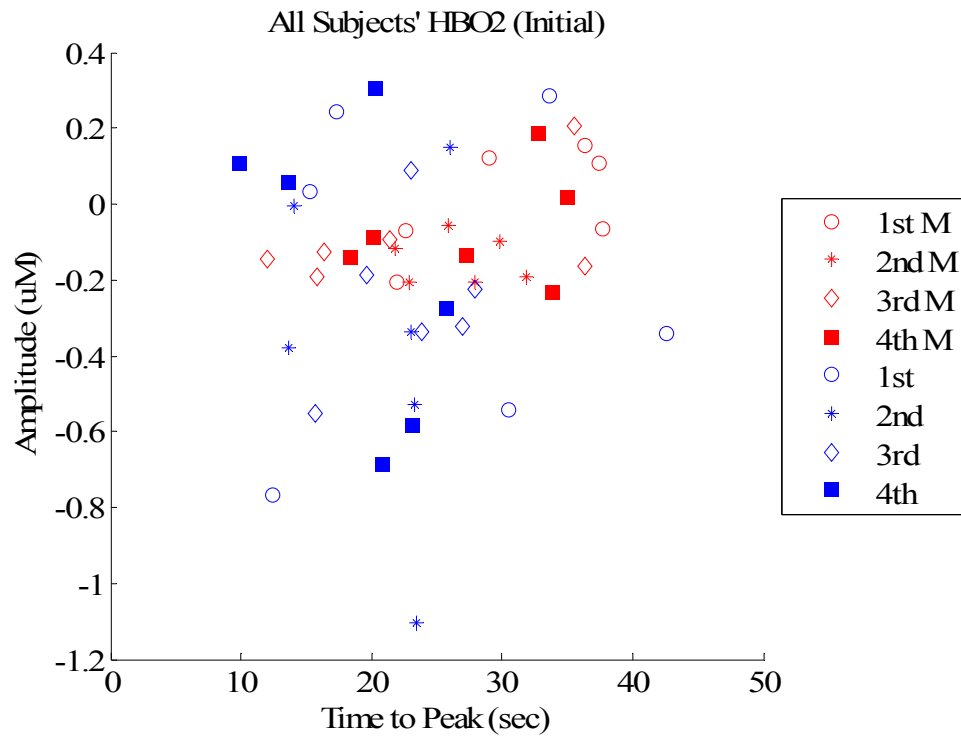


(a)

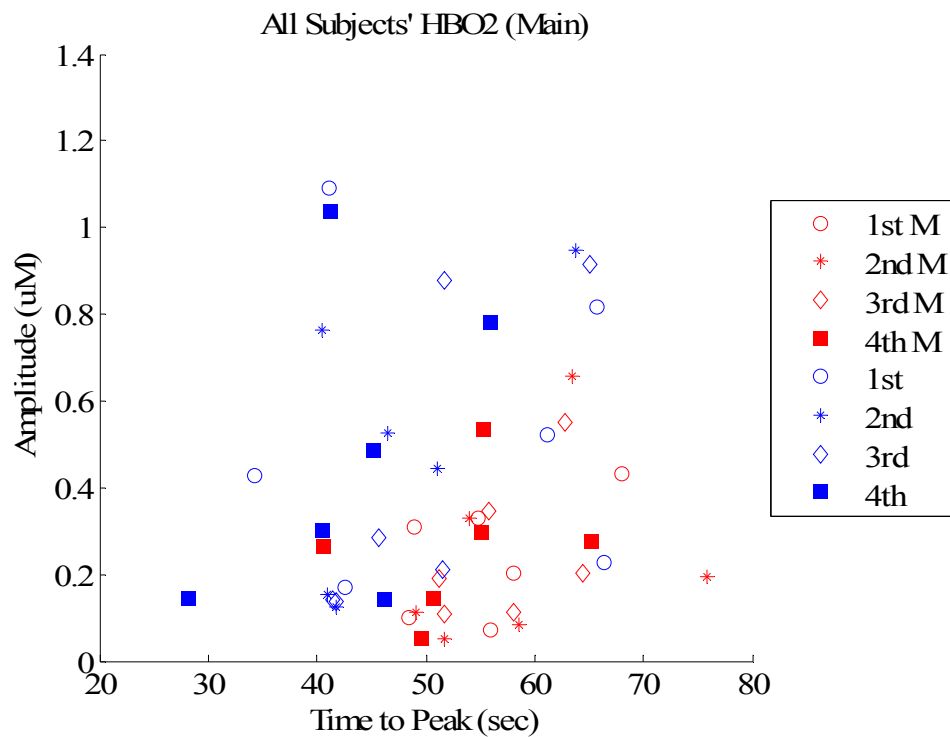


(b)

Figure A.2 [Hb] signal (a) main response and (b) recovery response scatter graphics for four consecutive breath holds from all subjects.



(a)



(b)

Figure A.3 [HbO₂] signal (a) initial response and (b) main response scatter graphics for four consecutive breath holds from all subjects.

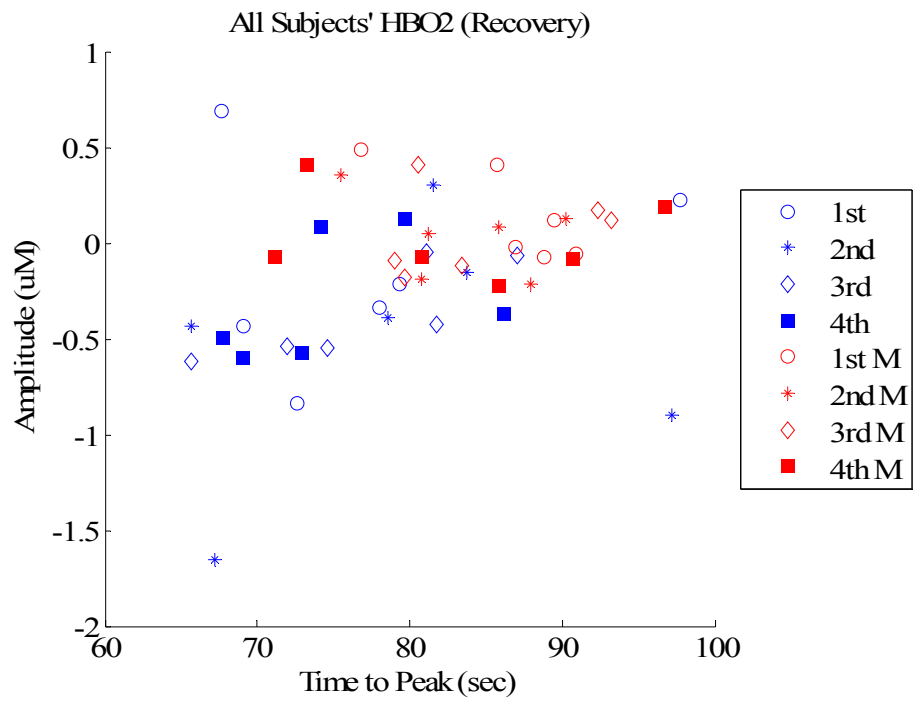


Figure A.4 [HbO₂] signal recovery response scatter graphics for four consecutive breath holds from all subjects.

REFERENCES

1. Edmeads, J., H. Findlay, P. Tugwell, W. Pryse-Phillips, R. F. Nelson and T. J. Murray, "Impact of Migraine and Tension-type Headache on Life-style, Consulting Behaviour, and Medication Use: a Canadian Population Survey," *Canadian Journal of Neurological Science*, Vol. 20, pp. 131-137, 1993.
2. Kemper, R., *Modelling Trigeminovascular Pain in the Unrestrained Rat: An Approach to a Better Understanding of Migraine Headache*, Ph.D. Thesis, Groningen University, 1999.
3. Bolay, H., U. Reuter and A. K. Dun, "Intrinsic Brain Activity Triggers Trigeminal Afferents in a Migraine Model," *Nature Medicine*, Vol. 8, pp. 136-142, 2002.
4. Michigan State University, Central Nervous System, http://kobiljak.msu.edu/CAI/Pathology/CNS_Infections_F/CNS_1c.html
5. Goadsby, P. J., and C. Boes, "Chronic Daily Headache," *Journal of Neurology, Neurosurgery and Psychiatry*, Vol. 72, pp. 2-5, 2002.
6. Headache Classification Committee of the International Headache Society, "Classification and Diagnostic Criteria for Headache Disorders, Cranial Neuralgias and Facial Pain," *Cephalalgia*, Vol. 8, Suppl. 7, pp. 13-96, 1988.
7. Stewart, W. F., A. Shechter and B. K. Rasmussen, "Migraine Prevalence: A Review of Population Based Studies," *Neurology*, Vol. 44, pp. 17-23, 1994.
8. Isler, H., "Headache Classification Prior to the Ad Hoc Criteria," *Cephalalgia*, Vol. 13 Suppl. 12, pp. 9-10, 1993.
9. Rose, F. C., "The History of Migraine from Mesopotamian to Medieval times," *Cephalalgia*, Vol. 15 Suppl. 15, pp. 1-3, 1995.

10. Ottman, R., S. Hong and R. B. Lipton, "Validity of Family History Data on Severe Headache and Migraine," *Neurology*, Oct, Vol. 43, pp. 1954-1960, 1993.
11. Baloh, R. W., "Neurotology of Migraine," *Headache*, Vol. 37, pp. 615-621, 1997.
12. Biondi, D. M., "Headache and the Mature Adult," *Headache*, Vol. 12, No. 2, 2001.
13. Hargreaves, R. J., and S. L. Shepherd, "Pathophysiology of Migraine - New Insights," *Canadian Journal of Neurological Sciences*, Vol. 26, Suppl. 3, pp. 12-19, 1999.
14. Loder, E., "What is the Evolutionary Advantage of Migraine?," *Cephalalgia*, Vol. 22, pp. 624-632, 2002.
15. Merck Medicus, Migraine Pathophysiology, http://www.merckmedicus.com/pp/us/hcp/diseasemodules/migraine/pathophysiology_sub.jsp
16. University of Manitoba, Anatomy of the Trigeminal Nerve, http://www.umanitoba.ca/cranial_nerves/trigeminal_neuralgia/manuscript/anatomy.html
17. Loyola University Chicago, School of Medicine, Trigeminal Nerve, http://www.meddean.luc.edu/lumen/MedEd/GrossAnatomy/h_n/cn/cn1/cn5.htm
18. Markowitz S., K. Saito and M. A. Moskowitz, "Neurogenically Mediated Leakage of Plasma Protein Occurs from Blood Vessels in Dura Mater but not Brain," *Journal of Neuroscience*, Vol. 7, pp. 4129-4136, 1987.
19. The Society for Neuroscience, Migraine and Serotonin Receptors, <http://apu.sfn.org/content/Publications/BrainBriefings/migrane.html>
20. Wolff, H. G., *Headache and Other Head Pain*, Oxford University Press, 1963.

21. Thomsen, L. L., "Investigations into the Role of Nitric Oxide and the Large Intracranial Arteries in Migraine Headache," *Cephalalgia*, Vol. 17, pp. 873-895, 1997.
22. Campbell, J. K., and R. J. Caselli, *Headache and Other Craniofacial Pain: Neurology in Clinical Practice*, Vol. II, Butterworth-Heinemann, 1991.
23. Leao, A. A. P., "Spreading Depression of Activity in the Cerebral Cortex," *Journal of Neurophysiology*, Vol. 7, pp. 359– 390, 1944.
24. Lauritzen, M., "Pathophysiology of the Migraine Aura: The Spreading Depression Theory," *Brain*, Vol. 117, Pt. 1, pp. 199-210, 1994.
25. Nedergaard, M., and A. J. Hansen, "Spreading Depression is not Associated with Neuronal Injury in the Normal Brain," *Brain Research*, Vol. 449, pp. 395– 398, 1988.
26. Andrew, R. D., T. R. Anderson, A. J. Biedermann and C. R. Jarvis, "Imaging and Preventing Spreading Depression Independent of Cerebral Blood Flow," *International Congress Series*, Vol. 1235, pp. 421–437, 2002.
27. Lauritzen, M., "Cortical Spreading Depression in Migraine," *Cephalalgia*, Vol. 21, Issue 7, pp. 757, 2001.
28. Lauritzen, M., "Cerebral Blood Flow in Migraine and Cortical Spreading Depression," *Acta Neurologica Scandinavica*, Vol. 76, pp. 1-40, 1987.
29. Afra, J., A. Mascia, P. Gerard, A. Maertens de Noordhout and J. Schoenen, "Interictal Cortical Excitability in Migraine: A Study Using Transcranial Magnetic Stimulation of Motor and Visual Cortices," *Annals of Neurology*, Vol. 44, pp. 209-215, 1998.

30. Aurora, S. K., B. K. Ahmad, K. M. Welch, P. Bhardhwaj and N. M. Ramadan, "Transcranial Magnetic Stimulation Confirms Hyperexcitability of Occipital Cortex in Migraine," *Neurology*, Vol. 50, pp. 1111-1114, 1998.
31. The Society for Neuroscience, "Migraines and Serotonin Receptors," *Brain Briefings*, February 1998.
32. Lechner, H., E. Ott, F. Fazekas and E. Pilger, "Evidence of Enhanced Platelet Aggregation and Platelet Sensitivity in Migraine Patients," *Cephalgia*, Vol. 5, pp. 89-91, 1985.
33. Kovac, K., F. Herman and J. Filep, "Platelet Aggregation of Migraineurs during and between Attacks," *Cephalgia*, Vol. 10, pp. 161-165, 1990.
34. Sanchez, M., "This Is Your Brain with a Headache," *Headache*, Vol. 12, 2001.
35. Toronov, V., E. Gratton and A. Webb, "Simultaneous Near-Infrared Spectroscopy and Magnetic Resonance Imaging of Functional Activity in the Human Brain," *Research Advances in Medical Physics*, Vol. 1, pp. 1-15, 2003.
36. Emir, U. E, *System Characterization for a Fast Optical Imager*, M.S. Thesis, Boğaziçi University, 2003.
37. Villringer, A., and B. Chance, "Non-invasive Optical Spectroscopy and Imaging of Human Brain Function," *Trends in Neuroscience*, Vol. 20, pp. 435-442, 1997.
38. Kurth, C. D., J. M. Steven, D. Benaron and B. Chance, "Near-infrared Monitoring of the Cerebral Circulation," *Journal of Clinical Monitoring*, Vol. 9, pp. 163-170, 1993.
39. Villringer, A., J. Planck, C. Hock, L. Schleinkofer and U. Dirnagl, "Near Infrared Spectroscopy (NIRS): A New Tool to Study Hemodynamic Changes during

- Activation of Brain Function in Human Adults,” *Neuroscience Letters*, Vol. 154, pp.101-104, 1993.
40. Hirth C., H. Obrig, J. Valdueza, U. Dirnagl and A. Villringer, “Simultaneous Assessment of Cerebral Oxygenation and Hemodynamics during a Motor Task: A Combined Near Infrared and Transcranial Doppler Sonography Study,” *Adv. Exp. Med. Biol.*, Vol. 411, pp. 461-469, 1997.
 41. Colier W. N., V. Quaresima, B. Oeseburg and M. Ferrari, “Human Motor-cortex Oxygenation Changes Induced by Cyclic Coupled Movements of Hand and Foot,” *Exp. Brain. Res.*, Vol. 129, pp. 457-461, 1999.
 42. Toronov, V., M. Wolf, A. Michalos and E. Gratton, “Analysis of Cerebral Hemodynamic Fluctuations Measured Simultaneously by Magnetic Resonance Imaging and Near-infrared Spectroscopy,” WA5, Proc. OSA Technical Digest, Biomedical Topical Meeting, 2000.
 43. Kato, T., A. Kamei, S. Takashima and T. Ozaki, “Human Visual Cortical Function during Photic Stimulation Monitoring by means of Near-infrared Spectroscopy,” *Journal of Cerebral Blood Flow Metabolism*, Vol. 13, pp. 516-520, 1993.
 44. Sakatani, K., S. Chen, W. Lichty, H. Zuo and Y. P. Wang, “Cerebral Blood Oxygenation Changes Induced by Auditory Stimulation in Newborn Infants,” *Early Human Development*, Vol. 55, pp. 229-236, 1999.
 45. Chance, B., Z. Zhuang, C. Unah, C. Alter and L. Lipton, “Cognition-activated Low-Frequency Modulation of Light Absorption in Human Brain,” *Proc. Natl. Acad. Sci.* Vol. 90, pp. 3770-3774, 1993.
 46. Wolf, T., U. Lindauer, U. Reuter, T. Back and U. Dirnagl, “Noninvasive Near Infrared Spectroscopy Monitoring of Regional Cerebral Blood Oxygenation Changes during Peri-infarct Depolarizations in Focal Cerebral Ischemia in the Rat,” *Journal of Cerebral Blood Flow & Metabolism*, Vol. 17, pp. 950–954, 1997.

47. Firbank, M., E. Okada and D. T. Delpy, "A Theoretical Study of the Signal Contribution of Regions of the Adult Head to Near-infrared Spectroscopy Studies of Visual Evoked Responses," *NeuroImage*, Vol. 8, pp. 69-78, 1998.
48. Boas, D. A., T. Gaudette, G. Strangman, X. Cheng, J. J. A. Marota and J. B., Mandeville, "The Accuracy of Near Infrared Spectroscopy and Imaging during Focal Changes in Cerebral Hemodynamics," *NeuroImage*, Vol. 13, pp. 76-90, 2001.
49. Chance, B., E. Anday, S. Nioka, S. Zhou, H. Long, K. Worden, C. Li, T. Turray, Y. Ovetsky, D. Pidikiti and R. Thomas, "A Novel Method for Fast Imaging of Brain Function, Noninvasively, with Light," *Optics Express*, Vol. 2, pp. 411- 423, 1998.
50. Pearson, R. K., "Outliers in Process Modeling and Identification," *IEEE Trans. Control Systems Techn.*, Vol. 10, pp. 55-63, 2002.
51. Akgul, C. B., B. Sankur and A. Akin, "Selection of Frequency Bands in Functional Near Infrared Spectroscopy," *Journal of Computational Neuroscience*, Vol. 18, 2005.
52. Toronov, V., M. A. Franceschini, M. E. Filiaci, M. Wolf, S. Fantini and E. Gratton, "Near Infrared Study of Fluctuations in Cerebral Hemodynamics during Rest and Motor Stimulation Spatial Mapping and Temporal Analysis," *Medical Physics*, Vol. 27, pp. 801-815, 2000.
53. Strik, C., U. Klose, M. Erb, H. Strik and W. Grodd, "Intracranial Oscillations of Cerebrospinal Fluid and Blood Flows: Analysis with magnetic resonance imaging," *Journal of Magnetic Resonance Imaging*, Vol. 15, pp. 251-258, 2002.
54. Guyton, A. C. and J. E. Hall, *Textbook of Medical Physiology*, W. B. Saunders Company, 1996.

55. Rajapakse, R. C., F. Kruggel and J. M., Maisog, “Modeling Hemodynamic Response for Analysis of Functional MRI Time-series,” *Human Brain Mapping*, Vol. 6, pp. 283-300, 1998.
56. Chen H., D. Yao and Z. Liu, “A Comparison of Gamma and Gaussian Dynamic Convolution Models of the fMRI BOLD Response,” *Magnetic Resonance Imaging*, Vol. 23, pp. 83-88, 2005.
57. Gordon K. S., “Nonlinear Regression,” in A. H. El-Shaarawi and W. W. Piegorsch (eds.), *Encyclopedia of Environmetrics*, Vol. 3, pp 1405–1411. Chichester: John Wiley & Sons, 2002.
58. National Institute of Standards and Technology, Engineering Statistics Handbook, <http://www.itl.nist.gov/div898/handbook/pmd/section1/pmd142.htm>